Schweizerische Eidgenossenschaft
Confédération suisse
Confederazione Svizzera
Confederaziun svizra

Eidgenössisches Departement für Umwelt, Verkehr, Energie und Kommunikation UVEK
Département fédéral de l'environnement, des transports, de l'énergie et de la communication DETEC
Dipartimento federale dell'ambiente, dei trasporti, dell'energia e delle comunicazioni DATEC

Bundesamt für Strassen
Office fédéral des routes
Ufficio federale delle Strade

Heat Exchanger Anchors for Thermo-active Tunnels

Ancrages échangeurs de chaleur pour tunnels thermo-actifs

Wärmeaustauschanker für thermo-aktive Tunnel

Ecole Polytechnique Fédérale de Lausanne
Thomas Mimouni
Fabrice Dupray
Sophie Minon
Lyesse Laloui

Mandat de recherche FGU 2009/002 sur demande de Fachgruppe Untertagebau (FGU)

June 2013 **1417**

Schweizerische Eidgenossenschaft
Confédération suisse
Confederazione Svizzera
Confederaziun svizra

Eidgenössisches Departement für Umwelt, Verkehr, Energie und Kommunikation UVEK
Département fédéral de l'environnement, des transports, de l'énergie et de la communication DETEC
Dipartimento federale dell'ambiente, dei trasporti, dell'energia e delle comunicazioni DATEC

Bundesamt für Strassen
Office fédéral des routes
Ufficio federale delle Strade

Heat Exchanger Anchors for Thermo-active Tunnels

Ancrages échangeurs de chaleur pour tunnels thermo-actifs

Wärmeaustauschanker für thermo-aktive Tunnel

Ecole Polytechnique Fédérale de Lausanne
Thomas Mimouni
Fabrice Dupray
Sophie Minon
Lyesse Laloui

Mandat de recherche FGU 2009/002 sur demande de Fachgruppe Untertagebau (FGU)

June 2013 **1417**

Impressum

Service de recherche et équipe de projet

Direction du projet
Lyesse Laloui

Membres
Thomas Mimouni
Fabrice Dupray
Sophie Minon

Commission de suivi

Président
Prof. Dr. Georg Anagnostou

Membres
Felix Amberg
Martin Bosshard

Auteur de la demande

Fachgruppe Untertagebau (FGU)

Source

Le présent document est téléchargeable gratuitement sur http://www.mobilityplatform.ch.

Table des matières

Résumé

La géothermie peu profonde représente un réservoir d'énergie important pour le chauffage et la climatisation des bâtiments. Les niveaux relativement bas de température rencontrés à faible profondeur dans le sol, entre 10°C et 20°C, requièrent l'utilisation de pompes à chaleur pour pouvoir utiliser la chaleur extraite du sol. Cet ensemble forme le système GSHP (Ground Source Heat Pump).

Différents types d'échangeurs avec le sol ont été développés pour optimiser les échanges thermiques, depuis les sondes géothermiques scellées dans un forage dédié et pouvant atteindre quelques centaines de mètres de profondeur, jusqu'aux géostructures complexes. En effet, le contact entre le sol et l'échangeur de chaleur peut être amélioré par les propriétés thermiques du béton d'une fondation tout en économisant le coût du forage. Les développements récents ont suggéré que l'installation de géostructures dans les tunnels serait aussi efficace.

La présente étude a pour but d'estimer le potentiel de l'usage des ancrages et clous de tunnels en tant qu'échangeurs de chaleur avec le sol environnant. La première étude porte sur une tranchée couverte dont les ancrages, maintenant les parois moulées, ont été thermiquement activés. L'étude de la tranchée couverte tient compte des fluctuations annuelles de température à la surface du sol à cause de la faible profondeur des ancrages. Des conditions non saturées sont aussi étudiées dans ce cas. En revanche, les implications mécaniques ne sont pas prises en compte car la faible profondeur de l'ouvrage fait que son confinement mécanique est négligeable. Ensuite, un tunnel foré a été modélisé. De par sa profondeur plus importante, le tunnel foré est supposé reposer dans un sous-sol saturé en eau et l'influence thermique de la surface du sol est négligée. Par contre, le confinement du tunnel du au poids du sol l'entourant n'est plus négligeable et les implications mécaniques de l'exploitation de la chaleur par les clous sont étudiées.

Plusieurs types de cycles d'exploitation ont été testés. L'extraction de chaleur est basée sur les variations de température extérieure de l'air afin de suivre une demande simplifiée d'énergie d'un bâtiment. Des cycles avec ou sans injection de chaleur pendant la période chaude ont été considérés. Tous les cycles d'exploitation ont été optimisés pour atteindre une limite de température dans le sol afin de ne pas le geler. Ensuite, les quantités d'énergie extractibles dans chacun des cas ont été comparées afin de déterminer un optimum selon les conditions.

Il a été trouvé qu'injecter de la chaleur pendant la période chaude est nécessaire pour assurer la durabilité du stockage de chaleur autour de la tranchée couverte. En revanche, le tunnel foré bénéficie d'une bonne recharge thermique naturelle qui rend le coût de l'énergie avec injection de chaleur plus cher que sans. De plus, les implications mécaniques significatives sur la structure du tunnel foré sont amplifiées lorsque de la chaleur est injectée. Ceci démontre l'importance d'un dimensionnement thermomécanique d'un tel système.

Enfin, il est estimé que l'énergie extractible de la tranchée couverte varie de 0.6 à 1.2 MWh de chaleur par an et par mètre de tunnel, selon si l'on considère ou non l'injection de chaleur. Le tunnel foré peut quant à lui produire de 2.8 à 4.0 MWh de chaleur par an et par mètre de tunnel.

Zusammenfassung

Flachgründige geothermische Energie ist eine wichtige Ressource zur Heizung und Kühlung von Gebäuden. Aufgrund relativ tiefer Temperaturen in niedriger Bodentiefe zwischen 10°C und 20°C werden sogenannte Bodenwärmepumpen benötigt, um die gewonnene Wärme zu verarbeiten.

Verschiedene Typen von Bodenwärmetauschern wurden entwickelt, um den Wärmeaustausch zu optimieren. Diese Systeme reichen von einfachen geothermischen Heizkreisen in Bohrlöchern mit Tiefen bis zu einigen hundert Metern bis zu komplexen Energiegrundbauten. Der Verbau von geothermischen Heizkreisen in Betonfundamenten erhöht einerseits die Wärmeaustauscheffizienz und benötigt andererseits keine weiteren Bohrlöcher. Jüngste Entwicklungen deuten an, dass die Anwendung des Konzepts der Energiegrundbauten im Rahmen von Tunnelbauten effizient sein sollte.

Die vorliegende Studie untersucht das Potenzial der Verwendung von Tunnelankern und Bolzen als Wärmetauscher mit dem umliegenden Boden. Zwei städtische Tunnelbaustrukturtypen wurden untersucht. Im ersten Beispiel wurde ein Tunnel nach offener Bauweise numerisch modelliert, dessen Abdichtungsschlitzwände mit langen Ankern gestützt werden. Dabei wurden der thermische Einfluss der Bodenoberfläche und der ungesättigte Bodenzustand in Oberflächennähe berücksichtigt. Der mechanische Einfluss der Wärmegewinnung auf den Tunnel wurde vernachlässigt, da der Tunnel frei verformbar ist. Im zweiten Beispiel wurde ein stättischer Bohrtunnel untersucht. Es wurde angenommen, dass der Boden allzeit gesättigt ist und thermische Schwankungen an der Oberfläche vernachlässigbar sind. Die mechanische Einwirkung des Wärmeaustausches auf die Tunnelstruktur wurde in diesem Fall hingegen berücksichtigt.

Verschiedene Typen von Wärmegewinnungszyklen wurden in diversen Konfigurationen getestet. Die Wärmegewinnung ist abhängig von der äusseren Lufttemperatur, die den Wärmebedarf definiert. Zyklen mit und ohne Wärmeeinspeisung wurden ebenfalls untersucht. Die Wärmegewinnungszyklen wurden optimiert, um ein Gefrieren des Bodens zu vermeiden. Aus dem Vergleich zwischen gewonnener und eingespeister Wärme in den verschiedenen Zyklen kann eine optimale Methode zur Wärmegewinnung bestimmt werden.

Den Berechnungen zufolge ist es im Falle des Tunnels nach offener Bauweise nötig, in der Wärmeperiode Wärme in den Boden einzuspeisen, da der natürliche Wärmezufluss nicht ausreichend ist, um die Wärmespeicherung nachhaltig zu sichern. Im Falle eines Bohrtunnels ist die Wärmeeispeisung eine teurere Lösung aufgrund der natürlichen, hohen Wärmeregenerierung. Desweiteren ist der mechanische Einfluss der Wärmegewinnung auf den Bohrtunnel während der Wärmeeinspeisung grösser. Diese Schlussfolgerung weist ebenfalls auf die Wichtigkeit eines thermomechanischen Entwurfs solcher Systeme hin.

Schliesslich wird die Wärmegewinnung im Falle eines Tunnels nach offener Bauweise auf 0.6 bis 1.2 MWh und im Falle eines Bohrtunnels auf 2.8 bis 4.0 MWh pro Jahr und pro Meter Tunnellänge geschätzt.

Summary

Shallow geothermal power represents an important energy resource for the heating and cooling of the buildings. Due to relatively low temperature levels encountered at shallow depths in the soil, between 10°C and 20°C, heat pumps are required to process the extracted heat, forming the so called ground source heat pump system.

Different types of heat exchangers with the ground were developed in order to optimize the heat exchanges, from simple geothermal loops grouted in boreholes reaching depths up to a couple of hundreds of meters to complex energy geostructures. Indeed, embedding geothermal loops within concrete foundation structures increases the heat exchange efficiency as well as it saves the cost of additional drillings. Recent developments suggested that applying the concept of energy geostructures to tunnel structures that are in contact with the ground should also be efficient.

The present study investigates the potential of using tunnel anchors and nails as heat exchangers with the surrounding soil. Two main structures of urban tunnels were investigated. A cut and cover tunnel, whose diaphragm walls are maintained with long anchors, was modelled first. Thermal influence of the soil surface and unsaturated conditions were taken into account because of the shallow depth of the tunnel body. Nevertheless, mechanical implications of the heat extraction on the cut and cover tunnel were neglected because of the low mechanical confinement observed on the structure. Then, an urban bored tunnel was investigated. Soil conditions encountered at this depth were assumed always saturated and the thermal influence of the surface was neglected. Mechanical implications of the heat exploitation were assessed because of the high confinement of the bored tunnel body induced by the soil weight.

Different types of heat exploitation cycles were tested for the different configurations. The heat extraction is based on the external air temperature in order to meet a simplified building heat demand. Cycles with and without heat injection were also investigated. All the exploitation cycles were optimized in order to reach a temperature threshold in the ground to prevent freezing it. Next, comparisons between extracted and injected heat of the different cycles allow drawing an optimum exploitation method.

It is found that injecting heat during the hot period is necessary for the cut and cover tunnel as the natural heat reload isn't high enough to ensure the sustainability of the heat storage. Conversely, the bored tunnel beneficiates from an increased natural heat reload, turning the heat injection into a more expensive solution. Furthermore, mechanical implications of the heat exploitation on the bored tunnel are found to be more significant when injecting heat. This shows the importance of a thermo-mechanical design of such a system.

Finally, considering heat injection or not, it is estimated that heat extraction ranges from 0.6 to 1.2 MWh per year and per meter of cut and cover tunnel, and from 2.8 to 4.0 MWh per year and per meter of bored tunnel.

Final report

1 Introduction

The growing problematic of energy has recently encountered two main crises. Prices of fossil energies are constantly increasing as they are rarefying while the trust in the nuclear industry suffered severe setbacks like the catastrophe of Fukushima in Japan. Green energies already emerging in the past decades now experience a rapid growth in interest. Early local use of renewable energies is now to be turned into large scale production in order to replace the conventional energy sources.

Geothermal power comprises a wide panel of solutions from large geothermal power plants feeding towns with electricity and utilizing deep geothermal wheels (up to several kilometers) to ground source heat pumps (GSHPs) providing heat for single houses and utilizing shallow heat exchangers (from a couple of meters to a couple of hundreds of meters). Shallow geothermal power turns out to be one of the next energy sources as it is available all around the globe and easily accessible, while deep geothermal energy depends more on geological conditions and is more difficult to reach.

Among the different solutions provided by geothermal power, shallow geothermal power seems to be the most adaptable to any type of region. Indeed, reaching shallow depths is not a problem in term of technology and cost. Shallow geothermal power would induce a decentralization of the energy production reducing considerably the energy dependence of insulated regions and valorising resources that are unemployed yet.

Shallow geothermal power can be achieved by directly embedding heat exchanger loops in the soil or by combining heat exchanger loops with foundations structures. The second solution forms the family of energy geostructures.

The most recent developments of energy geostructures leaded to investigate the insertion of absorber pipes in shallow tunnel structures. Thus, thermally activated structures could be tunnel linings, invert slabs or anchors/nails utilized to maintain the tunnel walls during the construction. But choosing the adequate structure should come out from a decision based on the in situ conditions, design of tunnel structure and cost-efficiency of the system. Thus, facing such a design problem, comparative studies should be carried out for different scenarios in order to define the optimum conditions for the different available solutions.

Therefore, this study deals with a particular solution proposed which is the heat exchanger anchor. This project aims to estimate the amount of heat one can expect to extract from such a system under reasonable service conditions in different scenarios. First, a review of different ground source heat pump systems is made in order to define the context of the study. Particular attention is paid to existing systems coupled with tunnel structures. Next, the method adopted for the present study is detailed. The different tunnel structures that are considered are presented as well as the different conditions that are investigated and the models that are chosen are detailed and justified. Finally, the numerical analyses are presented and their results are analysed. The different parts of the modelling such as the mesh and adopted boundary conditions as well as the numerical strategy are presented. The results of the finite element analyses are analysed in term of extractible energy under given conditions and the mechanical implications are investigated. An estimation of the energy cost is then carried out for the different configurations in order to classify the efficiency of the systems according to the in situ conditions.

2 Shallow geothermal power

2.1 Heat consumption in Switzerland

As an illustration of the energy market that geothermal power could affect, statistics from the Swiss Federal Office of Energy (OFEN) were analysed for the year 2010 [1]. The three different sectors of energy consumption (figure 1: households, tertiary sector and industry)

were analysed. The energy consumption was divided according to the energy source utilized and its purpose putting the emphasis on the energy utilized to produce heat.

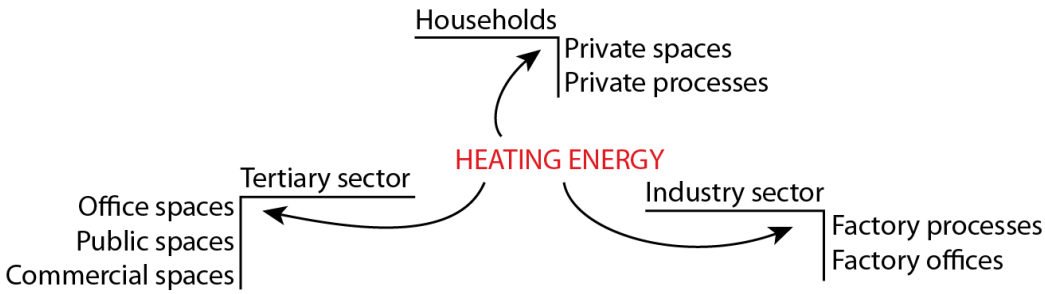

Figure 1: Diagram of the distribution of energy to the production of heat according the three distinct sectors: the households, the tertiary sector and the industry

It was found that about 85% of the total energy consumed by the Swiss households was dedicated to the production of heat (72.3% for the heating of space and 11.8% to the production of hot water) in 2010. But 75% of the energy used for the heating of space came from fossil fuels (54% from heating oil and 21.1% from natural gas), the production of hot water following the same trend (42.9% from heating oil and 20.2% from natural gas).

The tertiary sector exhibits the same tendencies as the households since their needs are similar. Thus, 53% of the total energy consumed in this sector was dedicated to heating of space and 8% to the production of hot water in 2010. All the fuel consumption of this sector was dedicated to the production of heat (87% for space heating and 13% for the production of hot water). Finally, about 10%of the totally consumed electricity was also dedicated to space heating.

The Swiss industrial sector is still based on strong consumption of fuels and electricity as more than the half of its energy consumption is destined to process heat and about one fourth to processes themselves (energy supply for machines). Nevertheless, the heating of space arrives in third position representing about 13% of the total industrial energy consumption.

From this analysis, it is obvious that developing new energy sources for the heating of space and production of the hot water is the most effective way to create significant impact on the energy consumption linked to the buildings in Switzerland and across the world. The first step that seems to come out from the above analysis is that heating the households and office/retail spaces is the first point that has to be impacted. Then, the developed technologies and systems could be extended to the industrial sector, having a lower but still not negligible impact.

In addition to its economic justification, shallow geothermal power is a clean energy source that only requires electricity to feed the heat pump and pumps during the heat exploitation. Thus, the carbon emissions linked to geothermal power reside in the fabrication of the polythene loops and heat pumps, their transportation and their installation plus the generation of electricity. Shallow geothermal power experienced great developments with vertical collectors that are now widely approved and utilized. But recent developments suggested that embedding vertical collectors in foundations structures (piles, diaphragm walls…) could increase the thermal efficiency of the system as well as its cost-efficiency. This particular type of collector, also called energy geostructures, utilizes the great heat capacity of concrete and allows saving the price of the drillings as the structural foundations are required anyway.

2.2 Ground source heat pump systems

2.2.1 General scheme

A Ground Source Heat Pump system (GSHP) is composed of heat pumps that are put in contact with the ground on one side and with a building to be heated or cooled on the other side.

The heat pump always needs to be in contact with a heat source and a heat sink. It then extracts heat from the heat source in order to inject it into the heat sink. The particularity of the heat pumps is that the heat source temperature is lower than the heat sink so that one must input external work to increase its temperature level. This is made thanks to the thermodynamic cycles that the refrigerant contained within the heat pump goes through. Indeed, the refrigerant is vaporized at the contact with the heat source and then compressed (transformation of electricity into work through the compressor and then heat through the refrigerant). Next, it is cooled down at the contact with the heat sink so that it transfers its heat to the heat sink and condenses. Thus, two modes of functioning can be adapted on GSHPs inverting the heat sink with the heat source.

Heat pumps utilized within GSHPs are usually *water-to-water* heat pumps. This means that the heat carrier fluid circulating within the heat exchangers between the heat pump and the ground as well as the one linking the building to the heat pump is water. *Water-to-air* systems can also be considered when floor heating systems are not possible but their efficiency drops significantly because of the low temperature level that GSHPs utilise.

The heat exchanger between the heat pump and the ground are numerous and each has its own specificities. Nevertheless, different attempts in order to classify them leaded to two main families that are the horizontal and vertical collectors, the vertical collectors reaching obviously deeper depths and temperature levels. Commonly, horizontal collectors are horizontal loops of pipe buried below the surface down to a couple of meters while vertical loops can reach a couple of hundreds of meters.

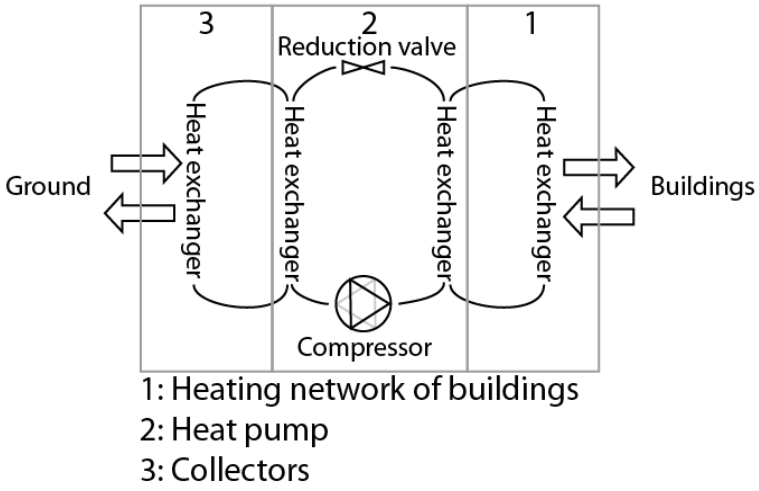

Figure 2: General scheme of a GSHP system for space heating purpose. The heat pump (2) is in contact with the building through the heating network (1) and with the ground through heat collectors (3).

2.2.2 Heating mode

For space heating, heat is extracted from the ground through the embedded collectors, processed with the heat pump and injected into the heating system of a building. In this mode, the heat source is the ground and the heat sink is the building. This mode induces a decrease of the soil temperature around the collectors.

In that configuration and for economic reasons, the coefficient of performance (COP) of the heat pump should not drop below 4 [2]. The COP is defined as the amount of power coming out form the heat pump divided by the amount of power provided:

$$\mathrm{COP} = \frac{\text{energy output after heat pump [kW]}}{\text{energy input for operation [kW]}} \quad (1)$$

Thus, with a ground temperature not decreasing below 0-5°C, output temperature after the heat pump remains at low levels between 35-45°C. This temperature level is enough for dis-

tributed heating networks such as floor heating with low temperature drops – between the inflow and return – of 5-6°C but is far from producing the required levels for conventional radiators with a fluid temperature reaching 80-90°C and a temperature drop between 10-20°C [3].Thus, heating houses with GSHPs also requires an adapted heating strategy with distributed heating networks and advanced thermal insulation to minimize to heat losses in order to keep the COP high.

More advanced GSHPs can produce temperature levels up to 65°C for hot sanitary water production (European standards) but, obviously, with a reduced COP.

For heating purpose, 30% to 50% of energy required by conventional air-air heat pumps can be saved with GSHPs [3]. The main reason is that the ground, during wintertime, exhibits a positive temperature between 8-15°C under European latitudes when the air temperature is close to 0 or even lower. Thus, the required energy to raise the temperature level of the extracted heat from the ground is reduced.

In conclusion, GSHPs are the most efficient heat pump systems for heating with COP going up to 4-5 but they require a specific type of heating network adapted to the low temperature levels that are produced and an efficient thermal insulation to minimize the heat losses.

2.2.3 Cooling mode

Depending on the region where buildings are installed, air conditioning demand can be greater than heat demand and GSHPs can then be turned into cooling machines. For regions where the cooling demand is low enough so that the heat pump can be by-passed during the hot period, direct cooling is generally used: the heating/cooling network of the buildings is directly connected to the ground collectors so that the heat carrier fluid is cooled at the contact of the ground and heated within the building. But, if the cooling demand increases, the heat pump becomes necessary and the building becomes the heat source of the system while the ground is the heat sink.

Under this configuration, the temperature of the ground increases when the building is cooled. Nevertheless, European norms indicate that the fluid temperature in cooling floors should not drop below 19-21°C to avoid dew within the floor. Again, an efficient thermal insulation coupled with an engineered air management will increase the efficiency of the whole system.

2.2.4 Seasonal exploitation

For buildings in regions where both heating and cooling demand are high, GSHPs are helpful thanks to the reversible heat pumps. This system is a simple vane allowing the selection of the heat sink and source depending on the season. Thus, during the hot season, the ground is the heat sink and the building the heat source and vice versa during the cold season.

The Seasonal Factor of Performance (SFP) is then defined to take into account the efficiency of the system in the two functioning modes – heating and cooling. The SFP is defined as [2]:

$$\mathrm{SFP}=\frac{\text{usable energy output of the energy system [kWh]}}{\text{energy input of the energy system [kWh]}} \tag{2}$$

The SFP will be used as the efficiency indicator in the rest of the study and typical values for GSHPs can vary between 3 and 4 [2, 3] taking into account seasonal variations of the COP. Indeed, the COP is mainly affected by the ground and building temperatures. Thus, at the beginning of the cold season, the ground exhibits a “high” temperature level (around 11°C) and the building temperature is not that cold so that the little heating demand is satisfied with a high COP. As the cold season goes on, the ground temperature decreases because of the heat extraction and the building temperature gets colder and colder. Thus, the COP decreases as more heating is required meanwhile the ground temperature drops. Then, at the end of the cold season when air temperature increases again, the COP starts increasing

again as less heating is required but the ground temperature still decreases. At the beginning of the hot season, the temperature of the ground should not drop below 0-5°C [2] and the cooling of the building starts. Thus, the ground temperature starts increasing and the cooling of the building is achieved with high COP values. But as the hot season goes on, the temperature of the ground increases and the cooling demand grows. Thus, the cooling of the building is achieved with a decreasing COP, and so on.
In conclusion, GSHPs are usable for the heating or cooling of the buildings with a high efficiency but at low temperature levels which requires efficient heating networks and efficient thermal insulation and air management.

2.3 Generalities on the existing systems

2.3.1 Open loop systems

Open loop systems employed in GSHPs are systems in which the heat carrier fluid is directly in contact with the ground heat source. This fluid can be air pumped through buried pipes or underground water pumped out from and rejected into an aquifer [4].

Open loop systems are the most inexpensive systems to install and are highly efficient but the impact on the environment might not be negligible as the fooling of the heat exchanger by organic matter has to be avoided with chemical inhibitors whose use is restricted [5] or mineral deposits have to be cleaned [2].

This type of system has been utilized with tunnels in Switzerland since the early 80's. The drained waters from the tunnel are processed through heat pumps to feed the neighbour building heating systems. The first tunnel utilizing the drained water was the tunnel of St Gothard (Tessin, Switzerland) where a flow of 7200 l/min naturally comes out from the tunnel at a temperature of 15°C. The water is processed through heat pumps and finally discharged at a temperature close to the natural level of the discharge watercourse (between 3°C and 6°C) providing great geothermal potential [6].

In conclusion, this type of system has inexpensive great efficiency but many factors have to be gathered to have a favourable environment and it is not generalizable to any region worldwide.

2.3.2 Closed loop systems

Closed loop systems are made of buried polythene pipes wherein a heat carrier fluid – water with antifreeze – circulates and collects the heat of the surrounding ground. Compared to the open loop systems, this system has a reduced efficiency because of the various heat exchanges occurring between the heat carrier fluid and the soil. First, the heat as to be carried out from the surrounding soil to the pipe walls through conduction or convection. Then, conduction through the wall carries the heat from the outside face of the pipe to the inside face of the pipes where heat is taken by the heat carrier fluid through forced convection. All the interfaces and walls add thermal resistances which reduce the thermal efficiency of the system. Nevertheless, close loop GSHP systems remain highly efficient.

The heat exchangers can be divided into two main families. Horizontal loops collect the heat from the top soil and are buried between 1 and 5 meters deep. They can also be buried below rafts where they reach greater depths [7]. Typical value of the heat exchange capacity for horizontal loops is 1kW for 40-80 meters of pipe.

Vertical loops are installed in narrow drillings but reach great depths from a tenth to several hundreds of meters but their installation is more expensive as it requires special drillings. They use the constant temperature level observed in the ground a tenth of meters below the surface while horizontal collectors are affected by the seasonal variations of temperature at the surface. Thus, their heat exchange capacity is increased compared to horizontal collectors as they reach greater volumes of soil and it reaches 20 to 50 m per kW [4, 8].

Vertical loops can even be divided into conventional borehole heat exchangers (BHEs) directly embedded into the soil and energy foundations [2].

The last category regroups all the foundation structures that are equipped with geothermal loops embedded within the concrete. Energy foundations are more cost-effective than conventional vertical loops as they are installed within foundation structures that have to be built anyway. Furthermore, their thermal efficiency is increased compared to conventional geothermal loops because of the great thermal properties of the concrete which is a better heat exchanger media with the ground [2]. The host structure can be a pile foundation, a diaphragm wall or even a floor slab. Thus, almost any type of structure can be equipped with energy foundations. Nevertheless, in order to ensure a correct cost-efficiency of GSHPs coupled with energy foundations, Brandl (2006) suggested that the foundation length should be at least 6 m deep.

2.4 Energy geostructures

Energy geostructures are the last more promising development of GSHPs as they might be applicable to any type of foundation structure. Their development is following the same trend as the already existing technologies, that is to say they are being adapted to different types of foundation structures in order to widen their utilization. The very first energy geostructure consisted in a floor slab equipped with polythene loops whose principle was rapidly transferred to pile foundations in 1984 and then to diaphragm walls in 1996 [2]. As equipped floor slabs are generally utilized with other types of energy geostructures, this section will only describe the technology of energy piles, energy walls and other energy geostructures linked to tunnels with different examples of projects.

2.4.1 Energy piles and walls

Many projects were carried out with energy piles both in Switzerland and across the world. Swiss success of energy piles can be illustrated by the Dock Midfield of Zürich airport built in 2003. This airport terminal was founded on 350 30-m long bored piles with large diameters (between 0.9 and 1.5 m) among which 300 were turned into geothermal piles. Each pile was equipped with 5 U-loops. Geothermal piles are utilized for heating and cooling the terminal. 85% of the heating is provided by the energy piles while almost the whole cooling demand is satisfied by direct cooling on the piles. For this particular project under European latitudes, the amount of injected heat during the cooling of the terminal is deliberately kept about 2 times lower than the extracted heat in order to preserve the high potential of direct cooling (SIA D 0190). Other examples of geothermal power applied to the Swiss tertiary sector (school, office space) can be found in the Swiss documentation SIA D 0190 as well as an application to the Swiss households.

European examples of projects including energy piles are numerous in the tertiary sector (for office, public or retail spaces). The One New Change building, built in 2010 in London (UK), is founded on piles among which 219 are geothermal piles. They contribute to the heating and cooling of 52’000 square meters of office and retail space. Another great European example is the Main Tower of Frankfurt (Germany) with more than 100 energy piles plus a diaphragm wall made of a hundred of heat piles. To illustrate the multitude of buildings in the tertiary sector that can include energy piles, Brandl (2006) quoted the Keble College in Oxford (UK) or the Arts Centre in Bregenz (Austria).

At the international level, no real comparison is available but a great interest from Chinese researchers through many numerical investigations implies that the developing China is about to widely utilize this technology. As suggested by Rawlings and Sykulski [9], geothermal foundations are widely utilized in Europe while vertical and horizontal geothermal loops are more accepted in the US for domestic use.

Finally, Brandl (2006) quotes one single example of factory utilizing energy piles which is a paper-processing plant. The extracted heat is utilized for the specific air conditioning that such an industrial production requires.

In conclusion, Europe is a pioneer in energy piles but their utilization is still confined to the heating and cooling of buildings of the tertiary sector (offices, retail spaces, public halls…) while conventional vertical or horizontal loops are preferred for heating and cooling the households.

Energy walls regroup heat pile walls, diaphragm walls and floor slab for the most commonly encountered structures. Their utilization is similar to the energy piles. The principle is still the same, that is to say absorber pipes are installed within the concrete of a foundation or underground structure. But the anchors required for maintaining retaining walls or diaphragm walls represent new opportunities for the development of energy geostructures. This will be more developed in the next section dedicated to thermo-active tunnels.

An example of activated floor slab is the slab of the Messe-Prater metro station of the U2 metro line in Vienna (Austria). The absorber pipes were deployed like a heating floor as shown in Figure 3.

Figure 3: Absorber pipes deployed above the floor slab of the U2 Messe-Prater metro sation (Vienna, Austria). From Adam and Markiewicz 2009.

2.4.2 Thermo-active tunnel linings

The last development of energy geostructures suggested that applying this technology to shallow tunnel structures that cross massive volumes of soil might be efficient. The technology opportunities available for this development are limited and Brandl (2006) clearly identified the different types of energy geostructures that can be considered.

Between the primary and secondary linings, there is the possibility to insert what Brandl (2006) calls “energy goecomposite”. This new generation of geosynthetics is further detailed in [10].

The secondary lining can be itself equipped with geothermal loops like floor slabs or diaphragm walls are. The advantage of this alternative is that the secondary lining elements are moulded with the absorber pipes before it arrives on the construction site. Connections between the different elements of the lining create the final network.

Inside the tunnel, the support of the road/railway structure on top of the tunnel invert (later called the invert slab) can be equipped with heat absorber pipes similarly to floor slabs.

Finally, anchors or nails are required to maintain the tunnel walls during the construction. These structures which are disconnected from the tunnel body after the construction could represent a great opportunity for energy geostructures.

Different example of realized projects in tunnels with different energy geostructures are given here-after.

Example of energy geosynthetics

Examples of thermo-active tunnels are concentrated in Austria, the pioneer European country in energy geostructures [11]. Different projects have utilized the above-mentioned technics.

A portion the Lainzer tunnel (the lot LT22), in Austria, was equipped with energy geotextile. This new generation of geotextile is equipped with a absorber pipes so that prefabrication is possible (Figure 4). The geotextile is placed between the primary and secondary linings [12].

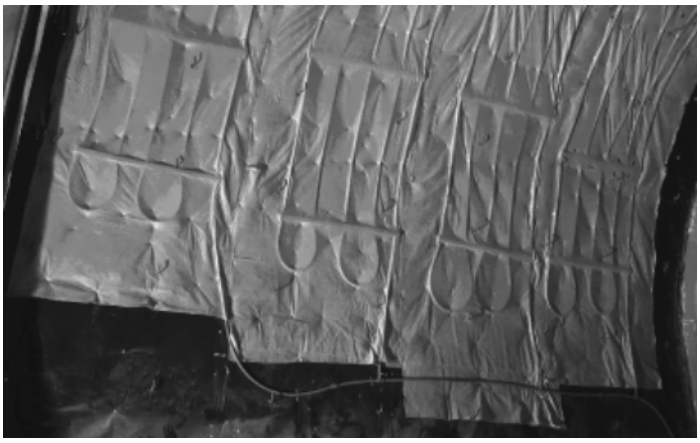

Figure 4: Example of an energy geotextile with the prefabricated sections and the collector pipe at the bottom. From Adam and Markiewicz 2009.

Example of thermo-active lining

Special Energy Lining Segments were design and fabricated for the secondary lining of a 54-m-long portion of the Jenbach tunnel (Austria) whose diameter is 12 m. The lining segments (Figure 5) were prefabricated including absorber pipes tightened to the reinforcing cage while moulding. Two snicks allow the connection of the elements and form “coupling pockets”. The connection of the elements (Figure 5) is achieved after their positioning by the Tunnel Boring Machine (TBM) whit a special device sealing both sides of a connection thanks to rings [13].

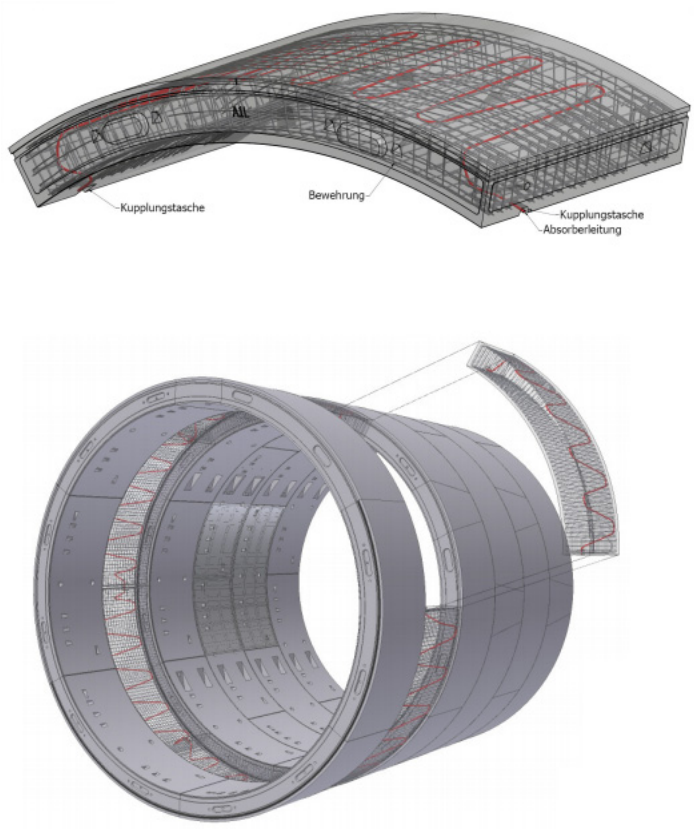

Figure 5: Example of an Energy Lining Element (top) and the assembling procedure (bottom), from Franzius (2011).

Example of activated invert slab

An example of thermally activated invert slab can be found in the Traborstrasse metro station (U2 Vienna metro line, Austria, Figure 6). Loops were deployed on top of the secondary lining before the invert slab was built [12].

Figure 6: Absorber pipes deployed on the invert slab in the Traborstrasse station tube, from Adam and Markiewicz (2009).

2.4.3 Heat exchanger anchors

A demonstration site of thermally activated anchors was also developed on a portion of the Lainzer tunnel, but with anchors not linked to the tunnel body. Being given the dimensions of anchors or nails, the coaxial arrangement of the hydraulic circuit turned out to be the most

effective [14]. Coaxial probes are inserted in the anchor/nail body (model R32N or R51L, see Oberhauser 2006). The inflow is entering the anchors/nail from the middle and the outflow is collected around the anchors/nail perimeter.

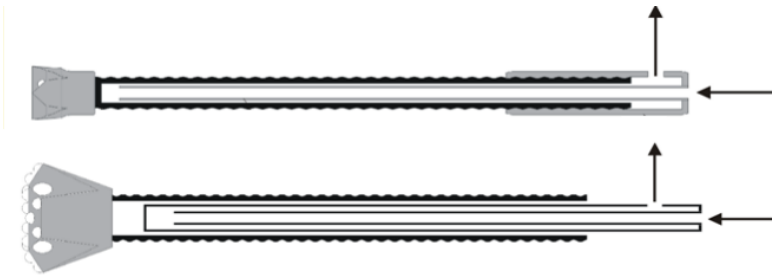

Figure 7: Anchor models utilized on the Wien demonstration site: R32N (top) and R51L (bottom), from [15].

Different configurations were tested on the demonstration site in Wien, Austria. Twenty one 12-m-long anchors/nails were installed in a sort of “hedgehog”. Their inclination with the horizontal was varying between 30° and 60° and the spacing between them was between 2 m and 4 m. 20 pieces where of the R51L kind while only one R32N model was left available for the test. Figure 8 shows the demonstration site in Wien, Austria.

Figure 8: Photograph of the demonstration site of thermally activated anchors in Wien, Austria. Hydraulic connections between the anchors are visible, from Adam (2008).

The different new developments of energy geostructures around the tunnel thematic show the wish to apply this rather young concept to the widest type of shallow underground structures. As Brandl (2006) reminds, the concept of earth-contact heat exchangers might be dedicated to shallow tunnels as the heat transport to the user is easier than for deep-seated tunnels. For the last category, if hot groundwater occurs, other technics such as collecting the drained waters might be more efficient and cost-effective.

Thus, shallow tunnel structures (the tunnel body plus the different underground stations and their foundations) activate a significantly larger quantity of geothermal heat than deep foundations. Nevertheless, the proximity between the different potential energy geostructures might lead to a reduction of the extracted heat. Thus, a design choice between the above-metionned solutions is required according to different factors.

The first factor is obviously the type of tunnel and its construction method. A cut and cover

tunnel will allow the installation of an activated slab floor, activated diaphragm walls and/or activated anchors while a bored tunnel allows installing energy geosynthetics, thermo-active lining elements, activated invert slabs and/or heat exchanger anchors. Depending on the in situ conditions, the dimensions of the different tunnel components may vary.

Therefore, the second factor is the heating/cooling system that must be combined to in situ thermal conditions. Indeed, great surface of heat exchanger might be required in some cases (e.g. a floor slab or diaphragm wall) while other situations could require narrow and spaced exchangers (anchors). This aspect has also to be linked to the available technology and its price. This stage should also include the design of the solicitation cycles underwent by the energy geostructures.

The third factor is then the cost-efficiency of the desired system. At this stage of development, heat exchanger anchors are not commercialized while finding rolls of polythene pipe is very easy. The installation of absorber pipes within reinforcing cages is also rather simple compared to installing anchors with a coaxial probe inside. Furthermore, connections between the different anchors to a collection line could occupy a significant space within the inner tunnel space (Figure 8). Utilizing thermo-active lining that is moulded in factory might be an alternative solution to the energy geosynthetics but the rather new technic requires specific connections between the lining elements.

In conclusion, the design of such thermo-active tunnels remains quite experimental and comparisons between the different solutions should be carried out depending on the different factors that were above-mentioned. The present study therefore proposes the analysis of heat exchanger anchors.

3 Method

This section is dedicated to the method utilized to investigate the thermo-mechanical behaviours of the tunnel structures equipped with heat exchanger anchors. First, and as suggested by the different factors influencing the design of thermo-active tunnels, two different types of shallow tunnel structures are investigated. A large panel of service conditions that can be underwent by each type of tunnel is analysed. Among the most important are the heat extraction/injection cycles the anchors are subjected to and the in situ conditions mainly represented by the nature of the soil and its water content. Next, the Thermo-Hydro-Mechanical (THM) approach that was adopted for this study is presented. The different models linked to the hydraulic, thermal or mechanical behaviours of the soil and tunnel structures are detailed as well as their couplings. Finally, the method utilised to estimate the cost of extracting and injecting heat into the ground through GSHPs is detailed.

3.1 The different tunnel structures investigated

The two shallow tunnel structures that were chosen to be representative for the widest range of encountered shallow tunnels are a cut and cover tunnel and a bored tunnel whose characteristics are detailed here-after.

3.1.1 Cut and cover tunnel

The cut and cover tunnel configuration corresponds to a top-bottom construction method in which the surface structures are removed during the whole construction of the tunnel. The space between the diaphragm walls is excavated until the desired depth. Then, the floor slab is built with the tunnel body on top. Joints are deployed all around the tunnel body and the remaining excavated space is backfilled. During the construction, anchors are required to maintain the diaphragm walls. As this type of tunnel remains really close to the soil surface, anchors remain close enough to the surface so that its thermal influence is not negligible.

For this case study, the anchors were designed with Rido software for a silty soil and with a longitudinal spacing of 3 m. The resulting design is made of height anchors per cross section which are 20 m-long and are inclined 20° below the horizontal (Figure 9).

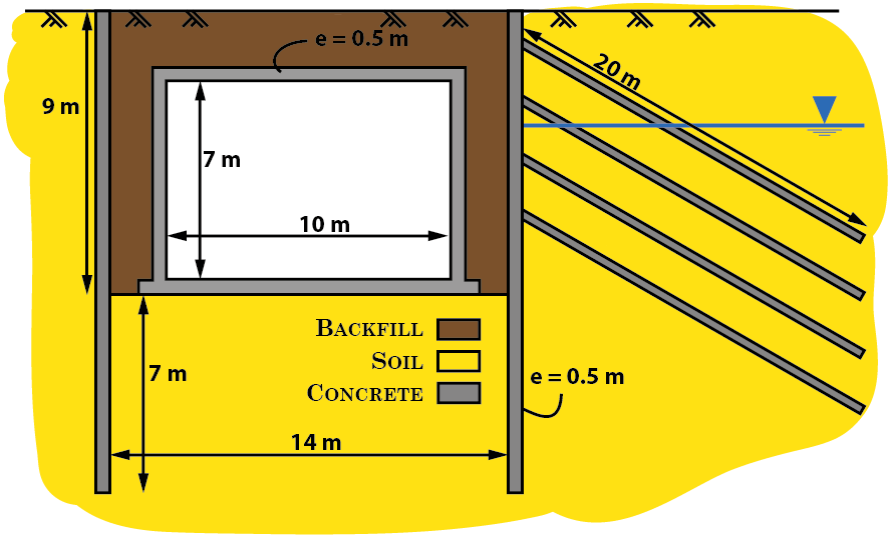

Figure 9: Scheme of the cut and cover tunnel. Backfill and Soil are the same materials since excavated soil is utilized as backfill.

3.1.2 Bored tunnel

The chosen configuration corresponds to an urban bored tunnel which remains close to the surface compared to tunnels crossing thick geological formations. Nevertheless, the surface is not expected to thermally influence the tunnel.

The tunnel design was inspired from the St Laurent M2 tunnel, in Lausanne, which is a road way tunnel. It is located 14 meters below the surface and the lining is maintained thanks to 24 3-meters-long bolts per cross section of tunnel. Cross sections are distant by 1.5 m. The tunnel lining is 0.5 m thick comprising a geotextile layer and its inner diameter is 11 meters.

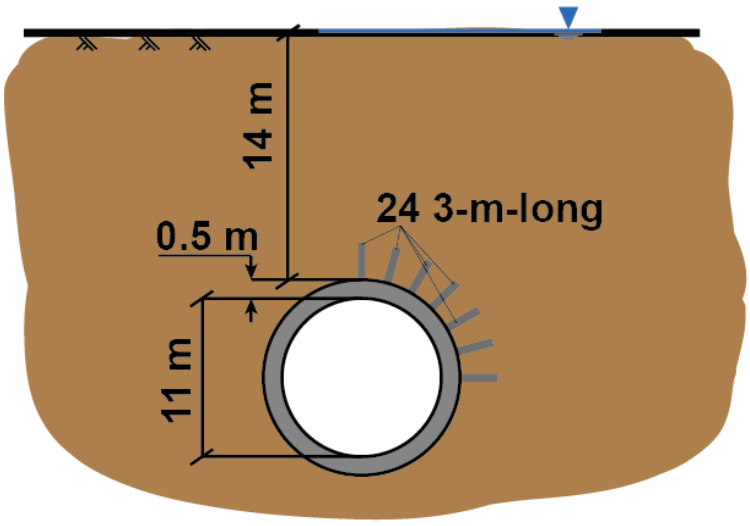

Figure 10: Scheme of the bored tunnel.

3.2 The different conditions investigated

The different conditions applied to the thermo-active tunnel regroup the thermal cycles which are applied to the heat-exchanger anchors and the type of soil in which the tunnel is embedded. The soil conditions are varying according to the type of soil and its water content.

3.2.1 Extraction/injection cycles

In a design process, the thermal solicitations the anchors will undergo are the result of the combination of the heat demand of the building and the chosen solution. In the present

study, the solution that is investigated is represented by heat exchanger anchors. Thus, the chosen solution is the designed anchor system. Nevertheless, as no particular demand is designed in this study, the adopted strategy was to vary the amplitude of the cycles in order to optimize the extraction and injection while fulfilling a given temperature criterion detailed hereafter.

The temperature criteria that was chosen is that the temperature in between two anchors, located in the most critical zone – thermally speaking – of the anchor array (e.g. in the middle of an array) should not drop below 273 - 274K (0-1°C). This condition of safety prevents:

freezing the buried water pipes close to the array of anchors, avoiding to cut water supply or damaging the buried pipes

freezing the soil to prevent frost heave and damages to the surface structures (roads…)

The criterion was set to 273 K for the cut and cover tunnel because no great mechanical implication is expected. Conversely, this criterion is raised up to 274 K for the bored tunnel to keep enough margins.

The adopted cycle for heat extraction and injection is unique for the whole study in order to keep the analysis rather simple. Its design is based on meteorological statistics recorded at Lausanne-Prilly weather station (Figure 11). Investigations were carried out on the sensitivity of the model to different climates encountered across Switzerland (Zürich for cold northern climate and Lugano for warmer climates next to the Italian border) and no significant differences were observed in the impact of the climate on the natural temperature profile in the ground. The statistics utilized were provided by the MeteoSuisse services (http://www.meteosuisse.ch). The statistics represent the average of the mean temperatures recorded between 1961 and 1990.

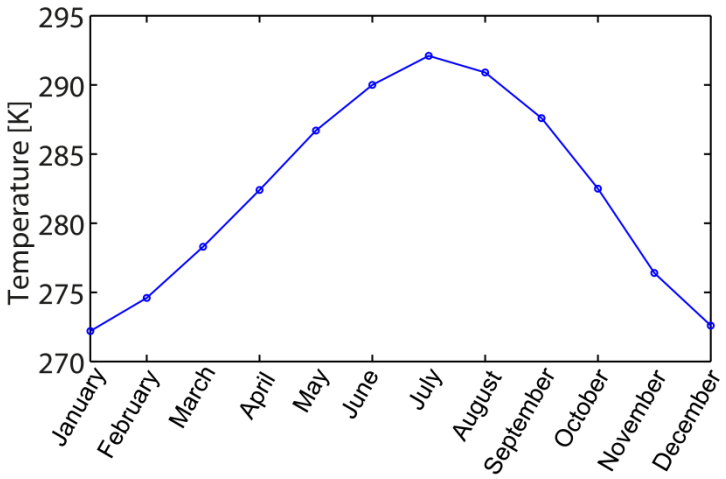

Figure 11: Mean of the monthly temperature averaged for the period from 1961 to 1990 at Lausanne-Pully weather station. Data from MeteoSuisse.

Adapting the heat extraction/injection on temperature data allows building a better scenario than using step functions. Indeed, heating systems installed in the buildings generally use a temperature gauge to monitor the outside air temperature. Thus, a threshold is fixed (between 10 and 13 °C) delimiting the domain when heating is required and obviously, the heating power is adjusted to the external temperature.

Thus, the shape of the thermal solicitation was design as a vertical mirror-like curve to the air temperature, leading to a heat flux multiplier function. Two different heat flux multipliers were defined (Figure 12):

- Ce, which stands for “Cycle extraction” defines a cycle where only heat extraction is considered

- Cei, which stands for “Cycle extraction and injection” defines a cycles where both heat extraction and injection are considered. Cei,i stands for a Cei cycle beginning by heat injection and Cei,e for the Cei cycle starting by heat extraction.

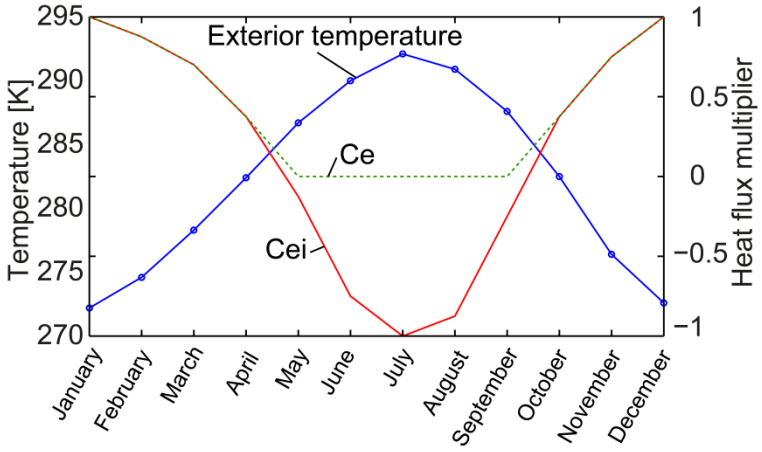

Figure 12: Curves for the heat flux multiplier in case of extraction only (Ce, dotted line) and extraction combined with injection (Cei, dashed line).

The really extracted and injected powers are built from the curves of heat flux multiplier by simple similarity multiplying them by a linear extracted or injected heat flux (in W/m of anchor), later noted P_0. Values of P_0 were determined by optimizing the Cei cycle for a silt soil under fully saturated conditions for both the bored tunnel and the cut and cover tunnel because it appeared that it is the most favourable configuration from a thermal standpoint. Thus, any other configuration (unsaturated silt, saturated or unsaturated clay, see next section) will lead to a reduced heat extraction potential.

3.2.2 Types of soils

As different types of soil can be encountered while digging a tunnel, the present study was carried out with different soil types. Two extreme cases were selected as they might be the most frequently crossed by shallow tunnels: clay and silt (Figure 13).

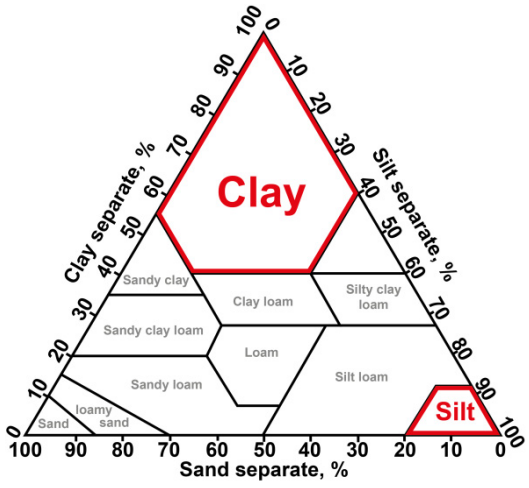

Figure 13: Soil texture triangle after the USDA.

The different soils are characterized by different mechanical and thermal properties. Structural and mechanical parameters are linked to the solid matrix forming the porous media. The void within the porous media is characterized by the porosity *n* and its value depends on the soil compaction.

In the present study, fluids filling the pore space can be either water or air. Thus, the water

content of a given soil may significantly affect its thermal properties [16]. Furthermore, as air thermal properties are lower than the ones of water, the more saturated a soil is, the more conductive and capacitive it is, thermally speaking.

If bored tunnels are generally deep enough so that their nails remain in a zone that is saturated all year long, cut and cover tunnels may suffer from desaturation of the surrounding soil. Thus, for the present study, the bored tunnel was only investigated in fully saturated conditions while the impact of a varying water table depth is analysed for the cut and cover tunnel. Nevertheless, intermittent saturation was not investigated but two different water table depths were chosen: 0m and -20m; remaining constant all year long.

In conclusion, the different soil conditions that are investigated for the present study are representative of the large soil conditions from silt to clay and from saturated to partially saturated.

3.3 Modelling of the tunnel and its environments

3.3.1 Hydraulic behaviour

The behaviour of water within the soil matrix is, in the present study, modelled through two main processes that are the fluid flow and the fluid retention capacity. The permeability quantifies the ability of a soil matrix to allow a flow under a hydraulic head gradient while the water retention characterizes the capacity of the pores to retain water.

Air behaviour through the soil matrix was not modelled and air pressure was assumed to be equal to 1 atmosphere everywhere there is air in the domain.

Fluid flow through a porous media

The fluid flows within porous media are described with the Darcy's law:

$$\underline{q_w} = -\frac{k_r.k}{\mu_w}.\left[\underline{\nabla} p_w + \rho_w.g.\underline{\nabla y}\right] \tag{3}$$

where p_w *is* the pore water pressure, $\rho_w.g.y$ represents the hydrostatic profile, y being the vertical coordinate. k, k_r and μ_w are the kinematic permeability coefficients and the water viscosity, and q_w is the Darcy velocity relative to the solid phase. The water dynamic viscosity μ_w (in Pa.s) describes the shear developed in water when it is put in movement. It is assumed linearly dependent on temperature (reference temperature T_0 = 273 K) with linear coefficients listed in Table 1:

$$\mu_w\left(T\right) = \mu_{w0}\left(1 + \alpha_{\mu_w}^{T}\left(T - T_0\right)\right) \tag{4}$$

Water flow also depends on the intrinsic permeability k (in m^2) and the relative permeability k_r (without unit). The intrinsic permeability is representative for solid matrix wherein fluid flows. Adopted constant values for clay and silt soils are listed in Table 2.

Relative permeability is used to take into account the reduction of the space utilized to build the flow of the water according to the degree of saturation of water in the soil matrix. Indeed, water will have less space to flow when the water saturation of the soil matrix is reduced and therefore its relative permeability will be reduced. Thus, the water relative permeability is always between 1 (for a saturated material) and 0 (for a dry material). The final permeability of the soil matrix is then given by the product of the intrinsic permeability k and the corresponding relative permeability k_r. Nevertheless, the relative permeability of water was set constant and equal to 1 for the present study, giving an upper bound of water flow.

Table 1: Water dynamic viscosity

Fluid	Dynamic viscosity μ_{i0} (in Pa s)	Dynamic viscosity coefficient α_{μ}^{T} (K^{-1})
Water	0.0013	0.011

Table 2: Intrinsic permeabilities of the investigated materials [17]

Soil	Intrinsic permeability k (in m^2)
Clay	10^{-15}
Silt	10^{-13}
Concrete	10^{-15}

Since no forced water flow is imposed in the present study, flow can only be triggered by porosity variation that could be either induced by soil deformation or by thermal expansion of water. In one hand, deformations of the soil lead to variations in porosity, increasing or decreasing the space where water is contained and creating pressure gradients. On the other hand, thermal expansion coefficient of water β_w was taken equal to $3.4.10^{-4}$ K^{-1} while air expansion is neglected (e.g. any variation of air pressure is assumed to diffuse rapidly). Furthermore, soil thermal expansion is taken equal to 10^{-5} K^{-1}.Thus, as the water expands or contracts more than the soil matrix, pressure gradients are generated when local temperature varies through water expansion and compressibility (water compressibility coefficient was taken equal to $1/\chi_w = 4.54\ 10^{-10}$ Pa^{-1}).

Water content of the soil

Pores in soils are generally filled by air or water. When pores are filled only with water, the soil is fully saturated. When air and water are present in the pores, the soil experiences unsaturated conditions. In unsaturated conditions, the water content of the soil can be linked to the matrix suction s thanks to water retention curves.

The water retention curve chosen in the present study is the Van Genuchten model [18] that describes the water content θ_w (or as chosen in the present study, the saturation degree $S_w = \theta_w / \theta_{sat}$ where θ_{sat} is the water content at saturation) of a soil according to the suction s ($h=p_w-p_a$) thanks to four parameters: m and Π that are defining the shape of the curve and S_{res} and S_{max} that are the residual and maximum saturation degrees, respectively. Everywhere the water pressure is greater than the air pressure, the degree of saturation is set to 1; elsewhere, it is given by equation (5). Π is also called the air entry pressure which represents the suction when the soil starts desaturating. The adopted model neglects the possibly hysteretic behaviour of water retention in some soils.

$$S_w(s) = S_{res} + (S_{\max} - S_{res}).\left[1 + \left(\frac{|s|}{\Pi}\right)^{\frac{1}{1-m}}\right]^{-m} \tag{5}$$

Values of the different parameters used to model the different soils are listed in Table 3. Selected values were chosen to be representative [19]. Thus, the air entry value Π of clay is taken 10 times greater than for the silt and its residual degree of saturation S_{res} is 2 times greater than for the silt.

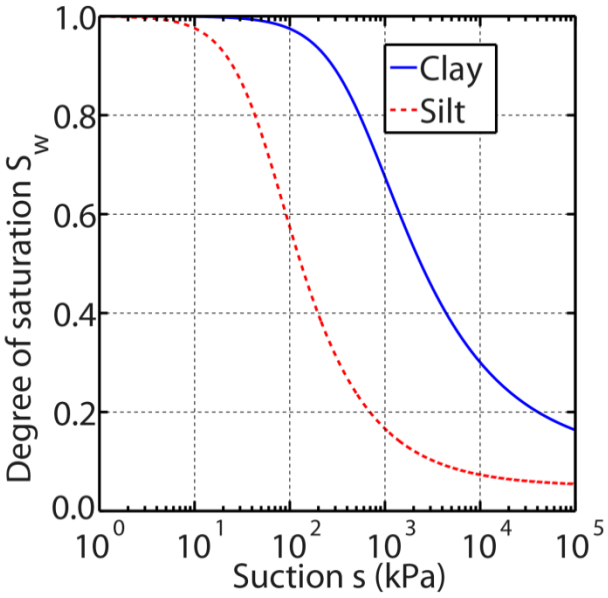

Figure 14: Representative water retention curves for clay and silt soils

Table 3: Van Genuschten parameters [19]

Soil	m	Π (kPa)	S_{max}	S_{res}
Clay	1/3	500	1	0.1
Silt	7/17	50	1	0.05

The water content is specified thanks to a water pressure profile that is in equilibrium with gravity (i.e. constant slope of $\rho_w.g$) and the water table depth is represented by the altitude where $p_a = p_w$.

Water mass balance equations

Since neither evaporation nor condensation is considered in the present study, the mass balance of water is expressed by:

$$\frac{\partial\left(\rho_w.n.S_w\right)}{\partial t} + div\left(\rho_w.\underline{q}_w\right) = 0 \tag{6}$$

where the density of water ρ_w is expressed as a function of the water pressure and temperature by:

$$\rho_w = \rho_{w0}\left(1 + \frac{p_w - p_{w0}}{\chi_w} - \beta_w\left(T - T_0\right)\right) \tag{7}$$

where ρ_{w0}, P_{w0} and T_0 are reference values.

3.3.2 Thermal behaviour

Heat propagation through soils involves conduction, radiation and convection for the most important part of heat transport. Liquid phase changes and ion exchanges can also be cited. But in unfrozen soils, the main heat transfer remains the conduction as convection requires large fluid flows to occur [20].

The heat equation, which is a balance of heat, is therefore utilized. This equation described the local temperature variation as the consequence of the heat diffusion, described by the Fourier's law, and the heat sink/sources Q_h present in the domain. The heat equation for a thermally isotropic medium is given by:

$$\rho.c.\frac{\partial T}{\partial t} = \lambda.\Delta T + Q_h \tag{8}$$

Where ρ, c and λ are respectively the density (in kg m^{-3}), the specific heat capacity (J kg^{-1} K^{-1}) and thermal conductivity (in W m^{-1} K^{-1}) of the media. Soils being multiphasic materials, bulk properties have to be defined from the individual properties of each constituent (air, water, solid) according to their proportions. The different proportions of the phases are determined with the porosity n of the porous media, relevant for the pore space within the solid matrix, and the degree of saturation in water S_w of the porous media, describing the proportions of water and air filling the pore space.

Thus, bulk quantities are derived with the mean geometric approach considering the volumetric fractions of each constituent:

$$\begin{aligned}\lambda_b &= (1-n).\lambda_s + n.S_w.\lambda_w + n.(1-S_w).\lambda_a \\ \rho_b.c_b &= (1-n).\rho_s.c_s + n.S_w.\rho_w.c_w + n.(1-S_w).\rho_a.c_a\end{aligned} \tag{9}$$

Where n is the porosity of the porous media, given in Table 5. s-cued quantities correspond to the solid phase, w-cued quantities correspond to the liquid phase and a-cued quantities are linked to the gas phase. Individual properties are given in Table 4.

Table 4: Individual thermal properties of the different constituents of the investigated soils [21]. Density is the grain density for solids and real density for gases and liquids.

	Thermal conductivity λ (W m^{-1} K^{-1})	Specific heat capacity c (J kg^{-1} K^{-1})	Density ρ (kg m^{-3})
Clay	2.42	732	2700
Silt	3.43	419	2700
Concrete	1.7	880	2500
Water	0.57	4186	1000
Air	0 (negligible)	1000	1.18

The bulk thermal diffusivity α_b compares the ability of a soil to conduct the heat and to store it:

$$\alpha_b = \frac{\lambda_b}{\rho_b.c_b} \tag{10}$$

Thus, the bulk thermal diffusivity is relevant for the thermal inertia of a porous media. The evolution of the bulk thermal diffusivity with the water content computed from equation (9) is plotted in Figure 15.

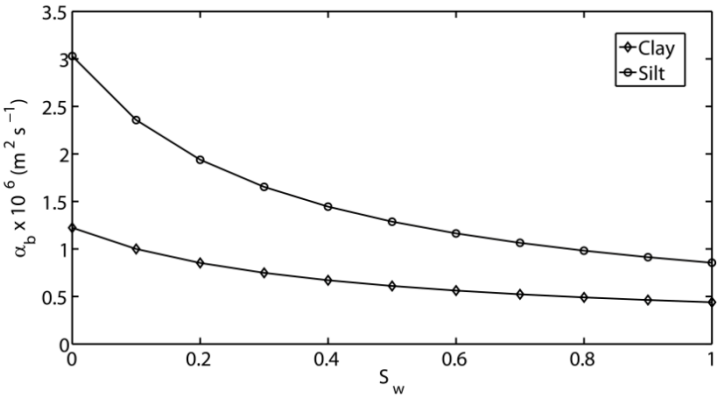

Figure 15: Evolution of the bulk thermal diffusivity with the water content for silt and clay soils.

The heat sources and sinks that can be found for the soil are the energy geostructure that are embedded within it and its surface. Indeed, in addition to the thermal cycles executed through the energy geostructures (see Figure 12), the soil undergoes the seasonal thermal wave since its surface is in contact with the air temperature. This phenomenon impacts the soil temperature down to 5-6 meters, depending on the soil thermal characteristics. In order to quantify this phenomenon, a characteristic depth of penetration z_0 in m, coming from the one dimensional (vertical) resolution of the heat equation for a semi-infinite medium, can be defined according to the duration τ of the thermal wave (e.g. one year) and the soil thermal bulk diffusivity α_b:

$$z_0 = \sqrt{\frac{\tau.\alpha_b}{\pi}} \tag{11}$$

In fully saturated conditions and based on Table 4, the value of z_0 for the silt soil is about 3 m while it is around 2.1m for clay. Thus, silt soil seems to be more sensitive to the surface influence. Furthermore, under dry conditions, the characteristics depths of silt and clay soils become respectively 5.51 m and 3.5 m. thus, the water content is expected to have a significant influence for the silt soil mainly, as clay retains well water.

Global energy balance equation

The global balance of energy is given by the heat equation that can be written as:

$$\frac{\partial S_T}{\partial t} + div\left(\underline{q_T}\right) - Q_T = 0 \tag{12}$$

where q_T the heat flux and Q_T a volumetric heat source or sink, S_T is the enthalpy of the medium (i.e. soil)given by:

$$S_T = \rho_b.c_b.\left(T - T_0\right) \tag{13}$$

where the product $\rho_b.c_b$ is given by equation (9), and the heat flux q_T is given by the Fourier's law:

$$\underline{q} = -\lambda_b.\underline{grad}\left(T\right) \tag{14}$$

where λ_b is given by equation (9). Injection equations (13) and (14) into equation (12) results in equation (8).

3.3.3 Mechanical behaviour

The soil and the concrete structures are assumed thermoelastic so that the parameters describing their mechanical behaviours are the elastic modulus E (in Pa) and the Poisson's ratio v which link the strain field $\underline{\underline{\varepsilon}}$ within the soil to the generalized effective stress field $\underline{\underline{\sigma'}}$ through the Hooke's law (equation (15)) as well as the thermal expansion coefficient α of the soil. The different parameters utilized to model the different soils are given in Table 5.

$$\underline{\underline{\varepsilon}} = \frac{1}{E}\underline{\underline{\sigma'}} - \frac{v}{E}\left[tr\left(\underline{\underline{\sigma'}}\right).\underline{\underline{I}} - \underline{\underline{\sigma'}}\right] + \alpha.\Delta T.\underline{\underline{I}} \tag{15}$$

Table 5: Mechanical and structural parameters [17, 22]

Specie	Elastic modulus E (Pa)	Poisson's ratio *v*	Porosity *n*	Thermal expansion α (K^{-1})
Clay	3.10^7	0.3	0.55	10^{-5}
Silt	3.10^7	0.3	0.45	10^{-5}
Concrete	3.10^{10}	0.2	0.2/0*	10^{-5}

*The porosity was set to 0 only for the analyses of the bored tunnel (see Section 4.2.1).

A first coupling between the thermal and mechanical behaviour is embodied by the thermal expansion coefficient of the solid or the liquid phase. The expansion of the gaseous phase is neglected in the present study because any air pressure variation is assumed to diffuse rapidly.

Momentum conservation equation

The global equilibrium of solids is given by:

$$div\left(\underline{\underline{\sigma}}\right)+\underline{b}=0 \tag{16}$$

where b is the body force vector and σ is the total (Cauchy) stress tensor. In the present study, the body force vector can be represented by the gravity and the behaviour of the soil is assumed to be governed by the generalized effective stress tensor σ' defined by:

$$\underline{\underline{\sigma}}=\underline{\underline{\sigma}}'-\left(S_w.p_w\right)\underline{\underline{I}} \tag{17}$$

Thus, equation (16) yields to:

$$div\left(\underline{\underline{\sigma}}'\right)-\underline{grad}\left(S_w.p_w\right)+\rho\underline{g}=0 \tag{18}$$

3.4 Estimating the price of the produced heat

A conventional heating/cooling system of a building coupled with energy geostructures can be described with the Sankey diagram presented in Figure 16. In a first time, let neglect the losses in order to simplify the writing of the equations.

The extraction energetic cost E_e is equal to the whole consumption of electricity given in equation (19), where E_{hp} represents the electricity consumed by the heat pump to process the extracted heat and $E_{e,g}$ is the energy utilized to extract the heat thank to the pumps of the system.

$$E_e = E_{hp} + E_{e,g} \tag{19}$$

Considering direct cooling in this scenario yields to the energetic cost of heat injection into the ground $E_{i,g}$ that is required to feed the pumps of the system.

Thus, considering injection or not, the total energetic cost E_f of a cycle is given by equation (20); $E_{i,g}$ being null when injection is not considered and the losses being neglected at first.

$$E_f = E_{hp} + E_{e,g} + E_{i,g} \tag{20}$$

Therefore, estimating the investment required for a type of cycle is achieved by multiplying the energetic cost E_f by the price of the energy P_e.

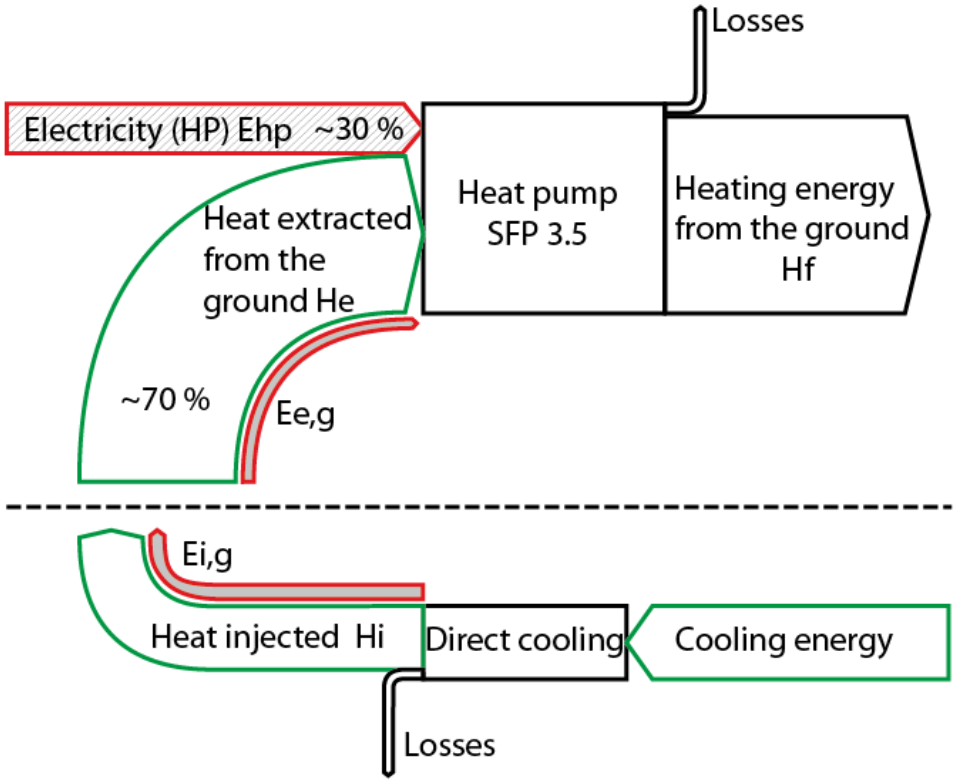

Figure 16: Sankey diagram of energies for the scenario with direct cooling and a SFP of 3.5. Electricity feeding the heat pump and the pumps of the system is the main running cost of the system. Cooling energy taken from the building and heat extracted from the ground are assumed "free".

The gain is represented by the final outcoming heating energy H_f which is given as a function of the SFP and H_e in equation (21).

$$H_f = \frac{SFP}{SFP-1} H_e \tag{21}$$

The energy E_{hp} required to process a given amount of energy H_e through a heat pump whose seasonal coefficient of performance is SFP is given in equation (22).

$$E_{hp} = \left(\frac{1}{SFP-1} \right) H_e \tag{22}$$

The energy input $E_{e,g}$ is generally taken into account into the COP or SFP determination as a part of the energy input [23]. Thus, it does not appear anymore in the following equations and will be embedded into the SFP value. Furthermore, $E_{i,g}$ is assumed proportional to the amount of injected heat H_i through the coefficient C_{pump}. Therefore, $E_{i,g}$ is given by:

$$E_{i,g} = C_{pump}.H_i \tag{23}$$

Thus, the energy cost in equation (20) can be expressed as a function of H_e and H_i as given in equation (24).

$$E_f = \left(\frac{1}{SFP-1} \right).H_e + C_{pump}.H_i \tag{24}$$

From the estimation of the produced heating energy H_f (equation (21)) and the invested cost estimated by multiplying the energetic cost E_f (equation (24)) by the energy price P_e, one can

estimate the final price of the heating energy outcoming from the system with equation (25). Comparisons between the prices obtained with and without energy injection can then be achieved:

$$P_h = \frac{E_f.P_e}{H_f} = \frac{\left[\left(\frac{1}{SFP-1}\right).H_e + C_{pump}.H_i\right].P_e}{\left(\frac{SFP}{SFP-1}\right).H_e} \tag{25}$$

One may see that if the injection is not considered, the price of the produced heat is directly linked to the SFP by:

$$P_h = \frac{P_e}{SFP} \tag{26}$$

The FEA analyses are used in that process to estimate the amounts of energy H_i and H_e that can be injected and extracted under different geotechnical constrains (avoiding frozen soils, bounded stress generation…).

More accurate analysis can be carried out considering the different efficiencies η at the different heat exchangers and energy converters. In the present study, the analysis with losses is made by estimating the additional costs that are required to produce the same amount of energy as without losses.

The first efficiency coefficient that is encountered accounts for the losses of extracted energy through the exchangers between the ground and the heat pump. An efficiency coefficient $\eta_{e,g}$ can be utilised to change H_e into $H_e/\eta_{e,g}$. Indeed, to collect H_e, one has to harvest $H_e/\eta_{e,g}$ in order to compensate the losses.

Similarly, injection efficiency $\eta_{i,g}$ can be utilised to correct the really injected heat H_i by $H_i/\eta_{i,g}$.

A converting efficiency η_C can be applied to the compressor of the heat pump converting electricity into mechanical work, correcting the consumed electricity E_{hp} into E_{hp}/η_C.

Finally, efficiencies of the pumps in the system can be accounted for by mean of a coefficient η_P changing $E_{i,g}$ into $E_{i,g}/\eta_P$. Thus, equation (25) would become:

$$P_h = \frac{E_f.P_e}{H_f} = \frac{\left[\left(\frac{1}{\eta_C.(SFP-1)}\right).\frac{H_e}{\eta_e} + \frac{C_{pump}}{\eta_P}.\frac{H_i}{\eta_i}\right].P_e}{\left(\frac{SFP}{SFP-1}\right).H_e} \tag{27}$$

It is interesting to see that injecting heat always increases the final price of the kWh which means that other criteria different from the gross price has to be taken into account. Indeed, this estimation does not fit any building energy demand or any power demand. Thus, injecting or not heat into the ground cannot be only based on the final gross price of the kWh of heat but also on the global demand in energy and power. In order to fully close the analysis of the prices, one may choose another energy source that would fill the gap in extracted energy between the cycles with injection and the ones without and then compare the new prices. For this purpose, we define an equivalent price P_{eq} which represents the price of 1 kWh of heat when the gap between the cycles with and without heat injection is filled. Let P_{fill} the price of 1 kWh of filling energy (fuel oil, gas, electricity…) in cts. Thus, the equivalent price is defined as:

$$P_{eq} = \left(1 - \frac{H_e(Cei) - H_e(Ce)}{H_e(Cei)}\right).P_h + \left(\frac{H_e(Cei) - H_e(Ce)}{H_e(Cei)}\right).\frac{P_{fill}}{\eta_{fill}} \tag{28}$$

where $H_e(Cei)$ is the amount of energy extracted during the cycle with heat injection and $H_e(Ce)$ the extracted energy when no injection is considered. η_{fill} takes into account the losses of filling energy while converting it into heat. For the sake of simplicity, η_{fill} is taken equal to unity in the present study (i.e. the conversion of the filling energy has an efficiency of 100%) so that P_{eq} represents a lower bound of the equivalent price.

Filling energies that can be considered (i.e. that can be utilized as a secondary heat source) and their prices P_{fill} can be oil whose price is 9.25 cts/kWh, gas whose price is 9.53 cts/kWh or type VI electricity whose price is 15.24 cts/kWh [24].

4 Numerical analysis

The different analyses are presented in this section. The investigations were carried out with the finite element code Lagamine [25-28]. The numerical strategy, describing the different steps of the modelling, is first detailed. Then, the numerical setup is described with the adopted mesh and the initial and boundary conditions. Finally, the results are presented.

4.1 Cut and cover tunnel

4.1.1 Numerical strategy

As the cut and cover tunnel remains close to the soil surface, yearly thermal wave influence has to be taken into account. Without any energy geostructure, the soil experiences seasonal temperature variations induced by the yearly air temperature variations. Thus, the first stage of modelling the cut and cover tunnel is to establish the natural thermal equilibrium between the air temperature and the ground. This stage (later called *Ini* for initialisation) is achieved by running a FEM analysis where only the soil surface temperature varies according to the yearly cycle described in Figure 11. From an initial condition of homogeneous temperature of 284 K everywhere in the domain, a modelled period of time of 30 years was enough to reach thermal equilibrium.

From this equilibrium, the anchors were activated by running different heating/cooling cycles and the influence of their utilization was analysed for a running period of 10 years.

Different configurations were investigated. Two different types of soil were analysed: clay and silt. For each soil, two different saturated conditions were chosen: water table at 0m or at -20m. Finally, for each saturated condition and each soil, three different heating/cooling cycles were investigated: one considering only heat extraction (Ce) and the two others considering heat injection (Cei) with one starting with heat extraction (Cei,e) and the other starting with heat injection (Cei,i). Thus, a total of 12 analyses were carried out about the cut and cover tunnel.

The mechanical behaviour of the structure was not considered as the anchors are disconnected from the structure after the construction of the tunnel and as the lack of vertical restraint and the low horizontal rigidity of backfill and wall compared to that of the tunnel body leave room for thermal strains.

4.1.2 Mesh and boundary conditions of the analyses

The mesh and the different components of the domain of the cut and cover tunnel are presented in Figure 17. The mesh was refined in the area surrounding the anchors. The domain is built around a symmetry axis. The mesh is made of 4988 nodes forming 1722 elements.

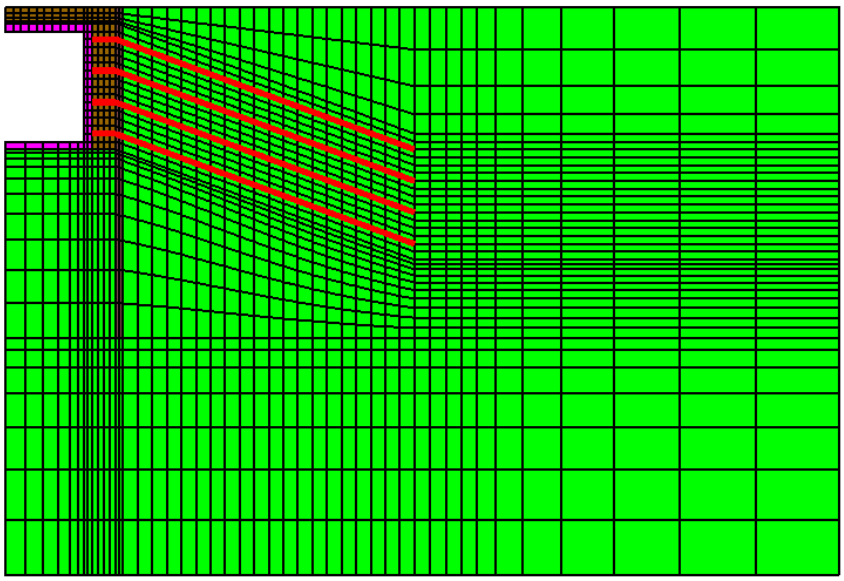

Figure 17: Mesh and the different components of the cut and cover domain. The soil is in green, the backfill in maroon and the anchors in red. The diaphragm wall is in dark maroon and the tunnel lining is in purple.

The boundary conditions applied to the domain limits are presented in Figure 18. They are divided into thermal and hydraulic conditions.

The temperature on the top boundary of the domain is imposed and varies in time according to the yearly temperature variations presented in Figure 11. The vertical boundaries of the domain as well as the tunnel walls are assumed adiabatic and the bottom of the domain is kept at 11°C to account for the geothermal gradient. Finally, a heat flux is imposed along the anchors.

Top, bottom and symmetry axis are impervious as well as the tunnel walls while the vertical right boundary of the domain has an imposed hydrostatic water pressure profile (Figure 18).

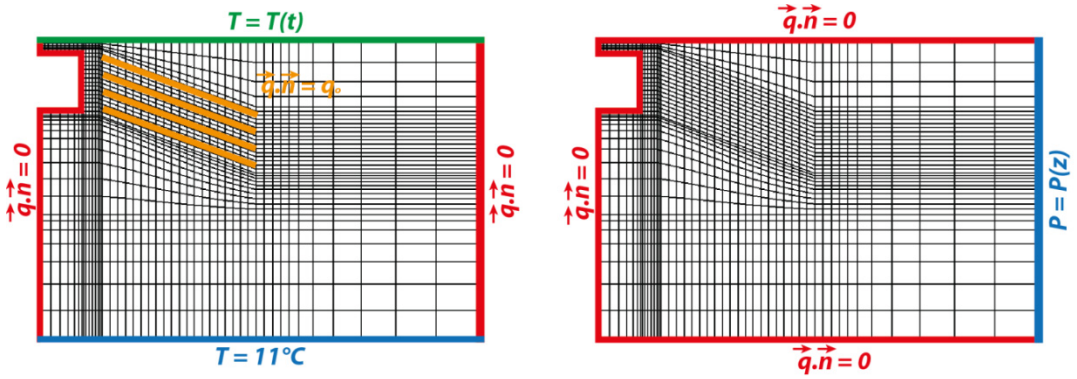

Figure 18: Thermal (left) and hydraulic (right) boundary conditions. In red are the zero normal flux conditions, in blue the imposed scalars and in green the time varying scalars.

In order to vary the water table depth, the pressure profile imposed on the right boundary of the domain is shifted downward but remains in equilibrium with the gravity. Thus, from this profile, the water content is derived thanks to the water retention curves described in equation (5).

4.1.3 Results

Extraction and injection of heat

The results of the optimization process lead to several conclusions. The optimization process

is based on the temperature time series measured at point 1 (Figure 19).

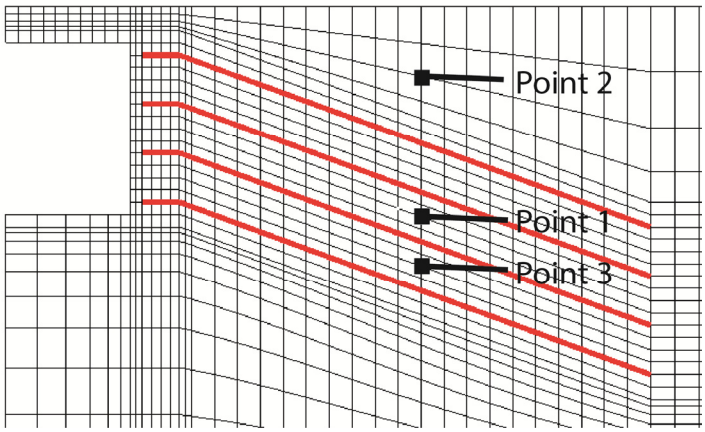

Figure 19: Points of measurements for the cut and cover tunnel analysis.

The optimized cycles are presented in Figure 20 for clay and in Figure 21 for silt. The corresponding temperature time series that were used for the optimisation are presented in Figure 22 for clay and Figure 23 for silt.

First, cycles with a water table at 0m and -20m for clay are the same (Figure 20 and Figure 22) because of the important water retention potential of clay (Figure 14). Thus, the water table depth does not significantly affect the water content of clay. Consequently, the bulk thermal properties of clay are not significantly modified (equation (9)) and the optimized cycles are similar.

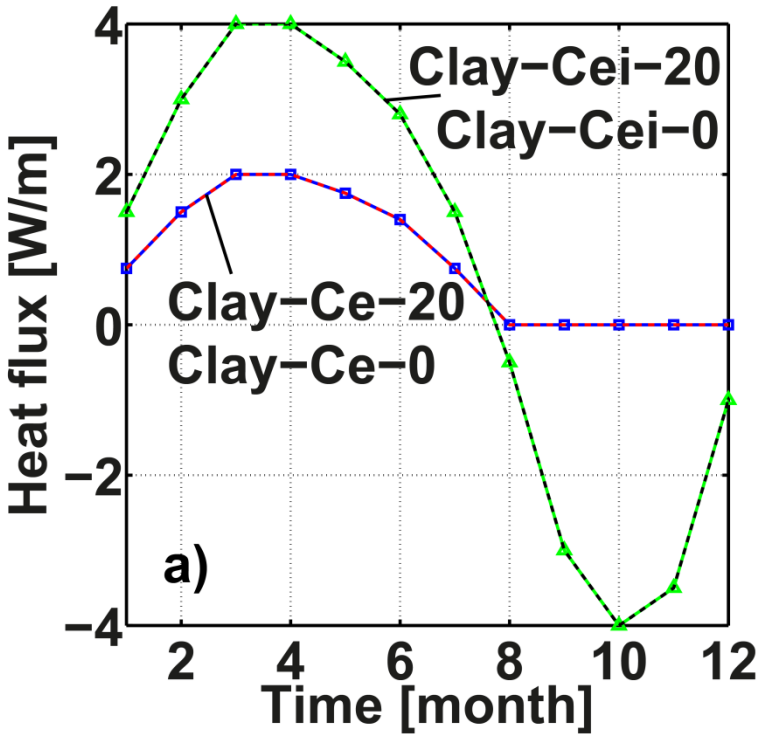

Figure 20: Optimised heat extract/injection cycles for clay soil. Ce-20 and Cei-20 are the optimized cycles for a water table at -20m.

Conversely, the water table depth has a great impact on the silt because of its low retention potential (Figure 21 and Figure 23). Thus, its water content varies a lot with the water table depth and its thermal properties are significantly modified.

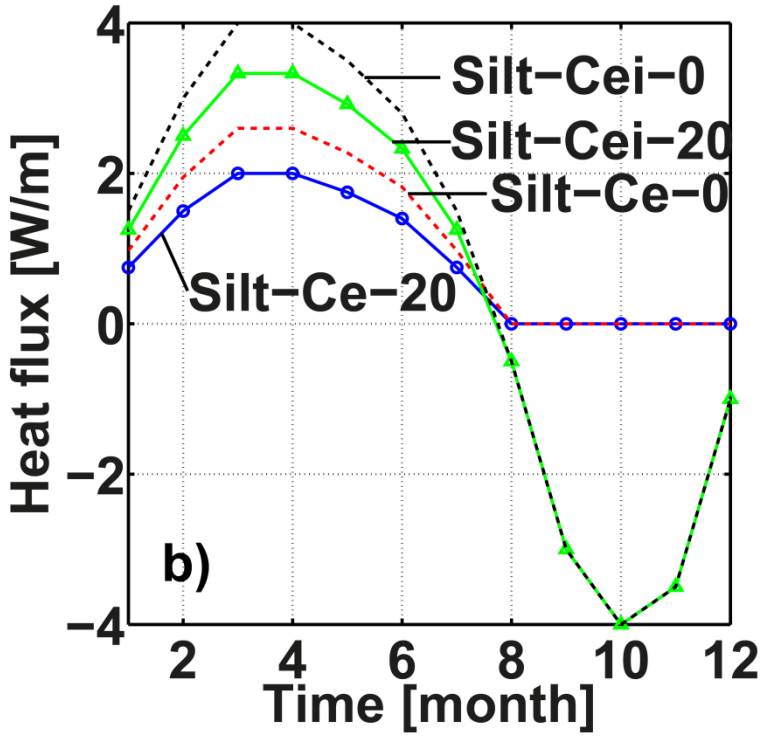

Figure 21: Optimised heat extraction/injection cycles for silt soil. Ce-20 and Cei-20 are the optimized cycles for a water table at -20m.

Clay is more affected by cycles without injection than silt: Ce-silt = 65% of Cei-silt while Ce-clay = 50% of Cei-clay and Ce-20-silt = 60% of Cei-20-silt while Ce-20-clay = 50% Cei-20-clay (Table 6). This is due to the fact that thermal diffusivity of silt is almost always greater than the one of clay (Figure 15). Thus, the thermal inertia of silt is less important than the one of clay (i.e. heat moves faster in silt than in clay) so that the natural heat reload is more efficient in silt than in clay. Nevertheless, heat capacity decreases as the water content decreases. Therefore, heat storage in unsaturated silt is less effective than in fully saturated silt so that the overall extractable energy is reduced when the water table is lower.

Table 6: Percentage of extracted heat compared to the most favourable situations

	Silt	Clay
Cei	100 %	100%
Cei-20	83%	100%
Ce	65%	50%
Ce-20	50%	50%

Temperature variations observed in silt with a water table at -20m are greater than the ones observed in fully saturated silt (Figure 23) because they are linked to the bulk thermal diffusivity and penetration depth concept: the greater the thermal diffusivity is, the better the temperature signal is transmitted farther. Thus, oscillations transmitted through the soil surface and mainly through the anchors are better transmitted in unsaturated conditions than in fully saturated conditions.

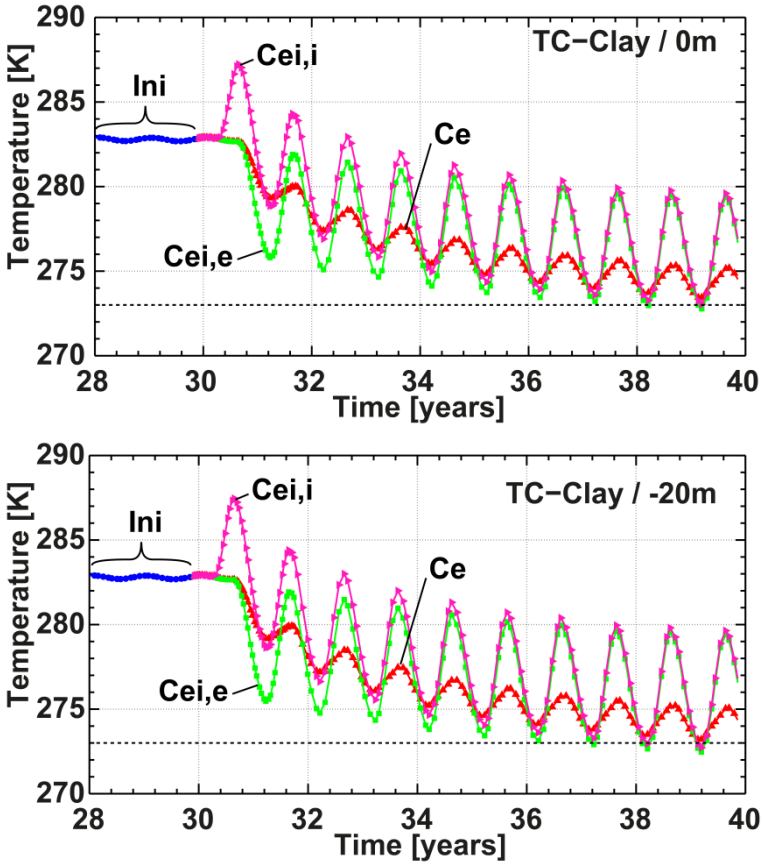

Figure 22: Time series of temperature at point 1 for the clay. Init represents the initialisation phase when the anchors are not activated. Ce represents the cycle where no injection is considered. Cei,e represents the cycle where injection is made but the heat exploitation starts by heat extraction. Cei,i is a cycle with injection but the heat exploitation starts by heat injection.

This phenomenon can lead to what is observed in Figure 23 during the first year within the unsaturated silt. As the heat exploitation starts by heat extraction (cycle Cei,e), the temperature in the middle of the anchors (point 1) drops below the water freezing threshold during the first year of exploitation. In the other hand, starting the heat exploitation by injection (cycle Cei,i) prevents the soil to freeze by increasing the initial temperature level before the first extraction occurs (Figure 23).

Furthermore, starting the heat exploitation by extraction or injection only affects the first 5 years. After that period, the temperature evolutions are the same for cycles Cei,e and Cei,i (Figure 22 and Figure 23).

Finally, injection overall allows greater heat extraction compared to passive heat reload (Table 6).

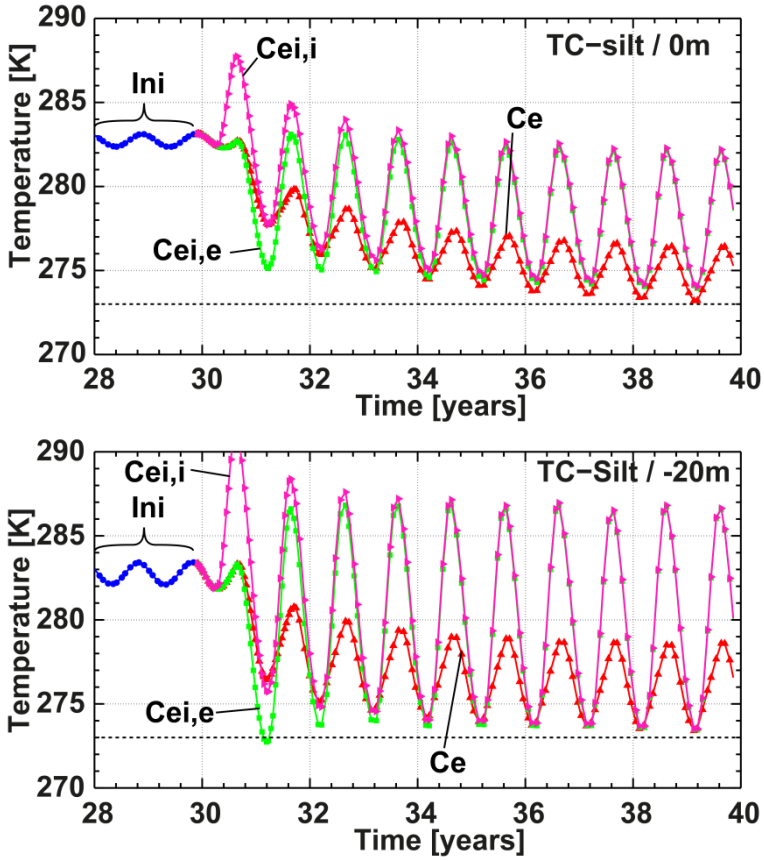

Figure 23: Time series of temperature at point 1 for the silt soil. Init represents the initialisation phase when the anchors are not activated. Ce represents the cycle where no injection is considered. Cei,e represents the cycle where injection is made but the heat exploitation starts by heat extraction. Cei,i is a cycle with injection but the heat exploitation starts by heat injection.

Evolution of temperature profiles were recorded along profiles 1, 2 and 3 (Figure 24).

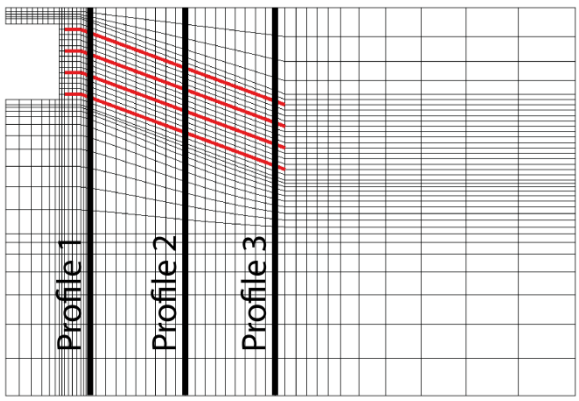

Figure 24: Location of profiles 1, 2 and 3.

The influence of the thermal solicitation of the anchors is represented in Figure 25 for the clay with a water table at the soil surface. The location of the anchors is clearly evidenced at the end of the heat injection (Figure 25 a, b and c) and the influence of heat injection and extraction is important from the surface to -20 m where the temperature never drops below 280 K.

Similarly, horizontal influence of the heat exploitation remains in a close vicinity of the anchors. The global impact on temperature of the soil can be observed in Figure 26 for the clay in fully saturated conditions (water table at the soil surface) undergoing Cei,e cycle, at the

end of the last extraction and injection phases.

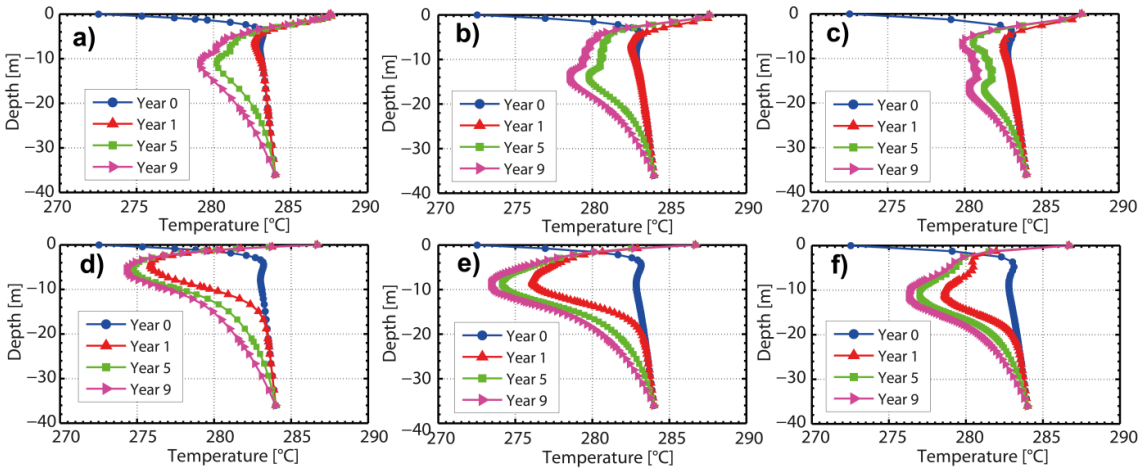

Figure 25: Vertical profiles of temperature through profile 1 (a and d), profile 2 (b and e) and profile 3 (c and f) at the end of heat injection (a, b and c) and end of extraction (d, e and f) for the fully saturated clay with Cei,e cycle.

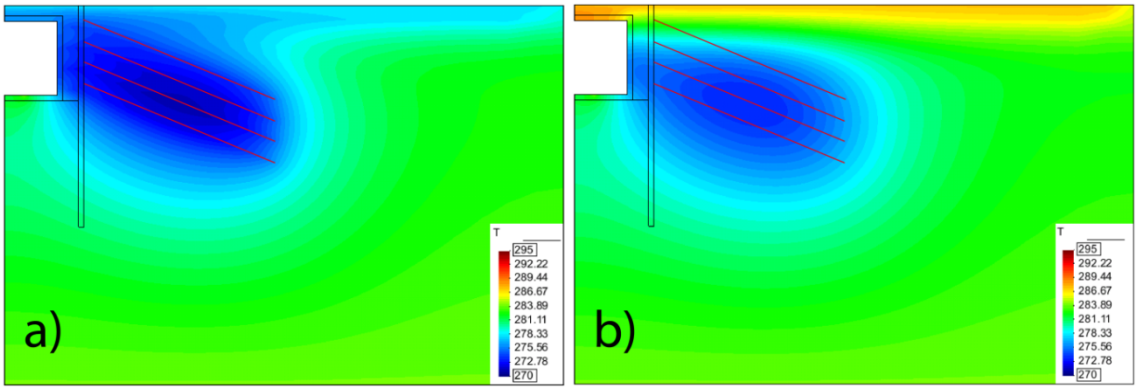

Figure 26: Contour fill of temperature for the fully saturated clay undergoing the Cei,e cycle, at the end of the last extraction (a) and last injection (b).

In conclusion, heat extraction may not be significantly affected by the water table depth within soils with high retention potential as their water content may not vary a lot, and consequently their thermal properties. Conversely, the water content of soils with weak water retention potential varies a lot as the water table moves and therefore their thermal properties significantly change.

Clay exhibits a less efficient natural heat reload (i.e. without heat injection) than silt as its thermal diffusivity is lower. Finally, heat exploitation considering heat injection should start by this phase in order to prevent soil freezing during the first year.

As the above analysis is mainly derived from a thermal standpoint, the different efficiencies listed in Table 6 should lead to utilizing the heat from the ground without considering heat injection. Nevertheless, this analysis never considers any energy demand or price linked to its utilization. Therefore, an estimation of the cost of the finally produced heat is presented in the following section.

Estimation of the energy cost

The extracted energy H_e and injected energy H_i into the anchors are estimated based on the optimized cycles (Figure 20 and Figure 21). The energy required to run the pumps of the system is arbitrarily assumed equal to 15% of the transported energy so that C_{pump} = 0.15. The price of the electricity P_e was taken from the OFEN statistics for 2011 when its averaged price was 16.2 cts/kWh [29]. The heat pump seasonal factor of performance (SFP) was as-

sumed equal to 3.5.

The estimations were carried out with and without taking into account the losses through the different efficiency coefficients. For simplicity, each efficiency coefficient was assumed equal to 95% when taking into account the losses.

The different estimations of energy and prices are gathered in Table 7. Compared to the statistics provided by the OFEN and the Heizen Mit Öl report [24], the prices that are estimated even with the losses are lower than the fuel oil or gas (between 9 and 10 cts/kWh) and type VI electricity– for heating – whose price was between 15 and 16 cts/kWh.

Equivalent prices P_{eq} indicate that the solution with heat injection remains the most economic under the assumptions made (Table 7).

Finally, the extractable heat from the ground H_e is converted from kWh per year and per meter of anchor into kWh per year and per meter of tunnel multiplying it by the length of anchor per meter of tunnel (Table 7). The cut and cover tunnel comprises height 21.75-m long anchors every 3 m so that there are 58 meters of anchor per meter of tunnel.

It is found that injecting heat leads to a cheaper energy for the considered configurations and geometry of tunnel (Table 7). Nevertheless, the influence of the estimation of losses is shown to have a significant effect on the final price.

The gain G in extracted energy while injecting heat varies according to the configurations because of the soil thermal conditions. This gain is expressed as the difference between the extracted energy when considering injection and the extracted heat without injection, divided by the injected heat:

$$G = \frac{H_e(C_{ei}) - H_e(C_e)}{H_i} \tag{29}$$

For the silty soil with a water table at -20 m, the energy gain G represents about 55% of the injected heat while it is equal to 57% with a high water table depth. The gain for the clayey soil does not significantly vary with the water table and it is equal to 84%. The impact of desaturation of silt has little impact on the gain. The differences in efficiency come mainly from the fact that the temperature variations are greater in silt than in clay (Figure 22 and Figure 23) because of the differences in thermal diffusivity (see Section 3.3.2). The thermal diffusivity is relevant for the propagation of thermal waves in soils and the greater it is, the less attenuated the thermal waves are [20]. In fully saturated conditions, thermal diffusivity of clay and silt are equal to 4.4×10^{-7} m^2/s and 8.5×10^{-7} m^2/s, respectively. Thus, temperature variations observed in silt can exceed the natural soil temperature by 3 to 4 degrees (when that water table is at -20m) while the temperature levels observed in clay always remain lower than 284K. Therefore, a part of the injected heat in silt diffuses away from the storage as its temperature level is greater than the rest of the soil. Conversely, the injected heat in clay remains within the heat storage and allows further heat to be transferred from the rest of the ground as its level remains lower than 284K.

In conclusion, it appears that for the given configuration of the cut and cover tunnel, the best heat exploitation requires cycles that consider heat extraction and injection. Indeed, the extractible heat ranges from 0.6 to 0.8 MWh per year and per meter of tunnel when no heat injection is considered while it ranges from 1.0 to 1.2 MWh per year and per meter of tunnel when heat is injected. In order to avoid freezing the soil during the first year of exploitation, the first use of anchors should start by the heat injection phase.

Table 7: Energies and costs computed from the results of the cut and cover tunnel analyses.

		Silt				Clay				Units
		-20		0		-20		0		
		Ce	Cei	Ce	Cei	Ce	Cei	Ce	Cei	
	He	7.41	12.02	9.63	14.46	7.41	14.46	7.41	14.46	(kWh/y/m of anchor)
	Hi	0.00	8.43	0.00	8.41	0.00	8.41	0.00	8.41	(kWh/y/m of anchor)
	Hf	10.37	16.82	13.49	20.25	10.37	20.25	10.37	20.25	(kWh/y/m of anchor)
	Ef	2.96	6.07	3.85	7.05	2.96	7.05	2.96	7.05	(kWh/y/m of anchor)
	Price	48.02	98.35	62.42	114.16	48.02	114.16	48.02	114.16	(cts/y/m of anchor)
Without losses	**Ph**	**4.63**	**5.85**	**4.63**	**5.64**	**4.63**	**5.64**	**4.63**	**5.64**	(cts/kWh)
	Peq (fuel oil)	**6.40**	-	**6.17**	-	**6.88**	-	**6.88**	-	(cts/kWh)
	Peq (gas)	**6.51**	-	**6.27**	-	**7.02**	-	**7.02**	-	(cts/kWh)
	Peq (Elec type VI)	**8.70**	-	**8.17**	-	**9.80**	-	**9.80**	-	(cts/kWh)
	Ef	3.3	6.7	4.3	7.8	3.3	7.8	3.3	7.8	(kWh/y/m of anchor)
	Price	53.2	109.0	69.2	126.5	53.2	126.5	53.2	126.5	(cts/y/m of anchor)
With losses	**Ph**	**5.13**	**6.48**	**5.13**	**6.25**	**5.13**	**6.25**	**5.13**	**6.25**	(cts/kWh)
	Peq (fuel oil)	**6.71**	-	**6.51**	-	**7.14**	-	**7.14**	-	(cts/kWh)
	Peq (gas)	**6.82**	-	**6.60**	-	**7.28**	-	**7.28**	-	(cts/kWh)
	Peq (Elec type VI)	**9.00**	-	**8.51**	-	**10.06**	-	**10.06**	-	(cts/kWh)
	Hf	**602**	**976**	**782**	**1175**	**602**	**1175**	**602**	**1175**	kWh / y / m of tunnel

Cpump = 0.15 | SFP = 3.5 | Pe = 16.2 cts/kWh |P(oil) = 9.25 cts/kWh | P(gas) = 9.53 cts/kWh | P(Type VI Elec.) = 15.24 cts/kWh [24]

4.2 Bored tunnel

4.2.1 Numerical strategy

The bored tunnel is assumed to be deep enough so that the thermal influence of the soil surface is neglected and the soil is assumed always saturated. Indeed, as estimated with equation (11), the characteristic penetration depths remain smaller than 6 m while the crown is 14 m below the soil surface.

Conversely to the cut and cover tunnel, the mechanical behaviours of the soil and tunnel structure are investigated because of the depth of the structure and the higher confinement level of the surrounding ground.

The first phase consists in modelling the tunnel excavation and the installation of the lining with the “convergence-confinement” method [30, 31]. This method is based on the reduction of nodal forces along the excavation perimeter as the initial mesh already comprises the excavation boundaries.

First, nodal forces around the virtual excavation are imposed to balance the soil weight along the inner perimeter of the future lining. Next, the nodal forces are reduced to a given ratio λ in a given period of time, defining an unloading rate v_λ (in s^{-1}). In the present study, the reduction of the nodal forces prior to the tunnel lining was taken equal to 70% (i.e. λ = 0.7) of the initial nodal forces in order to obtain sufficient vertical displacements generated by the excavation itself that would not be significantly affected by the virtual rise of the whole tunnel after the activation of the lining. Indeed, “when a lining is constructed during excavation, the subsequent unloading within the lining results in a desire of the complete tunnel to move upward, with a corresponding reduction in ground surface settlements. In a soft clay, this upward movement may be so significant as to cancel out all the ground surface settlement occurring before the lining construction” [30]. The first unloading was carried out over 6 days resulting in a quite high unloading rate $v_\lambda = 1.35.10^{-6}$ s^{-1} [32].

At the end of this phase, the lining is then activated by giving the lining elements the properties of concrete. Next, the nodal forces are reduced to zero (i.e. $\lambda = 1$) in 50 more days so that the lining carries the remaining weight of the soil [33].

Being given the relatively high unloading rate during the phase prior to lining installation [32] and the low permeability of the considered soils (Table 2), the excavation perimeter is assumed impervious and it was chosen that it would not act as a drain (porosity set to zero). Indeed, considering a waterproof tunnel which is not acting as a drain gives a higher bound of the stress levels developed around the lining [34] and keeps the design method conservative. Finally, the anchors are thermally activated and both thermal and mechanical implications are analysed.

The analyses are carried out thanks to records made along different profiles and at different points (Figure 27). Points 1, 2 and 3 are located on the tunnel extrados while points 1’, 2’ and 3’ are on the tunnel intrados. Point 4 is located in the most critical area for temperature evolution which is between two nails.

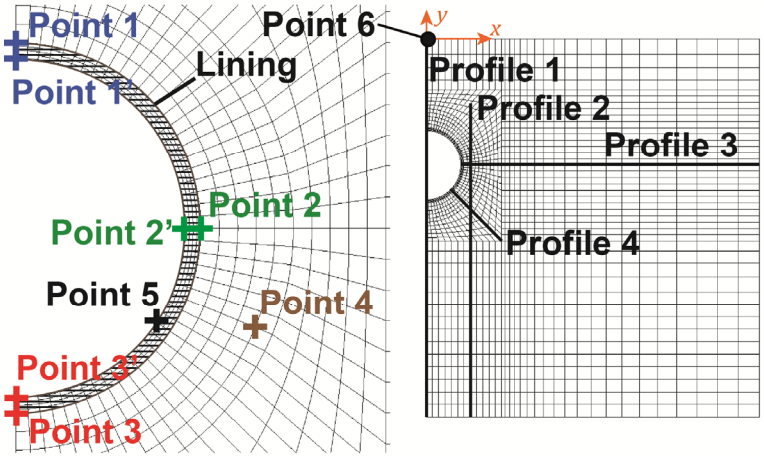

Figure 27: Location of the points and profiles used for the analyses for the bored tunnel.

4.2.2 Boundary conditions of the analyses

The mesh and the different elements utilized to model the bored tunnel are represented in Figure 28. The lining is represented with 4 layers of elements so that the stresses and strains that are developed can be correctly estimated. The mesh is made of 5385 nodes defining 1728 elements.

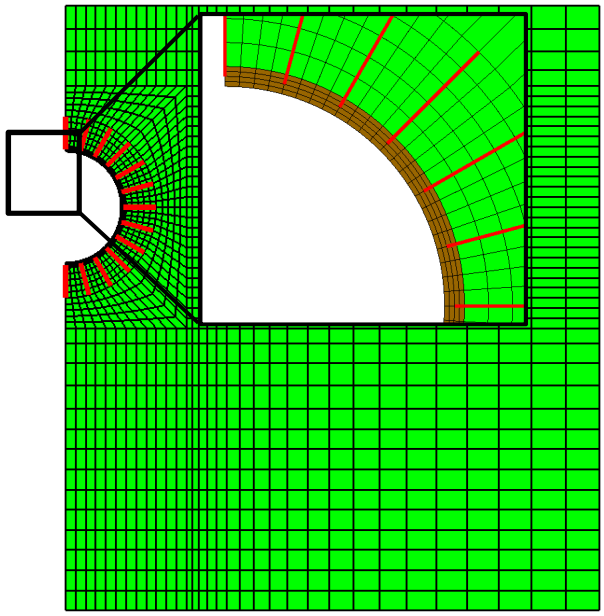

Figure 28: Mesh and the different components of the bored tunnel domain. The soil is in green and the anchors in red. The lining is in brown.

Horizontal displacements are blocked on the vertical boundaries of the domain except along the inner face of the tunnel lining. Vertical displacements are blocked at the bottom boundary of the domain. Temperature is fixed along the top and bottom boundaries as well as on the tunnel lining and the right boundary. Heat flux is set to zero on the axis of symmetry. Water pressure is fixed according to a hydrostatic profile on the right vertical boundary while all the other boundaries are set impervious (Figure 29).

The excavation forces are applied along the intrados of the future lining (in brown in Figure 28).

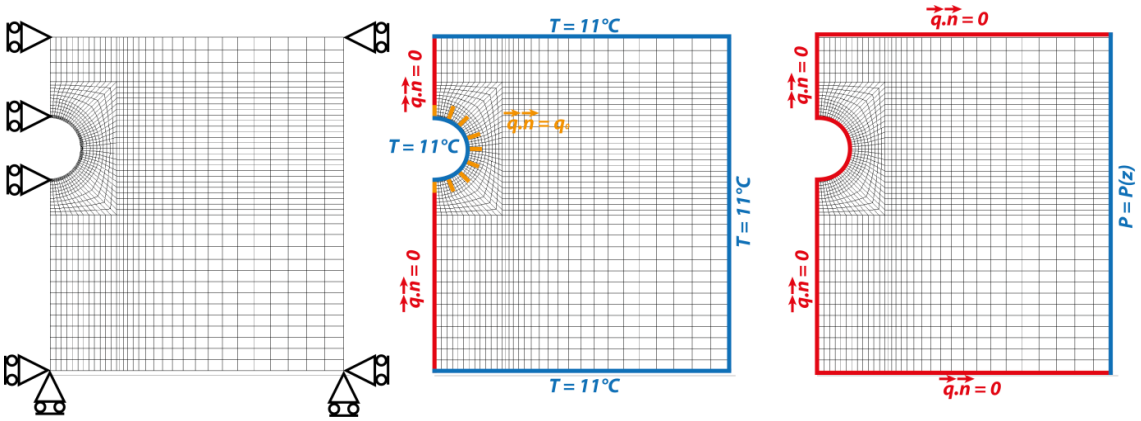

Figure 29: (Left) Mechanical, (middle) thermal and (right) hydraulic boundary conditions for the bored tunnel.

4.2.3 Results

First phase: tunnel excavation

Vertical displacements observed along profiles 1 and 2 (Figure 27) are presented in Figure 30. The part above the tunnel settles while the part below it rises. Those displacements are attenuated as the profile is farther from the tunnel axis. The major part of the vertical displacements occurs prior to the lining construction. Next, the general upward movement of the tunnel discussed in Section 4.2.1 is clearly observed in Figure 31 where points 1, 2 and 3 show similar behaviours.

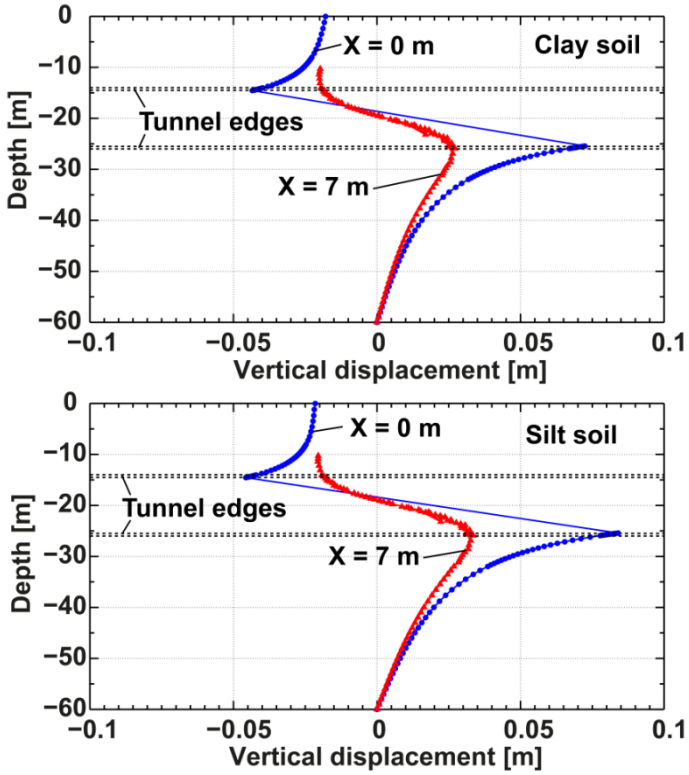

Figure 30: Profiles of vertical displacement at the end of the excavation along Profile1 (X=0m) and Profile2 (X=7m) for clay (top) and silt (bottom) soils

The unloading carried out in the confinement-convergence method induces a consolidation process in the soil. The efforts within the unloaded area are first transmitted to the pore fluid which is less compressible than the soil matrix and creates pressure gradient. Thus, water flows from the unloaded area towards areas where the pore water pressure is lower, transmitting the efforts to the soil matrix. As seen in Section 3.3.1, this process is driven by the

Darcy's equation that links the fluid flow to the hydraulic gradient observed within through the permeability coefficient. Equation (3) clearly evidences that the greater the permeability is, the greater the flow is, being given a hydraulic gradient. Therefore, the consolidation process is faster in the silt than in the clay and with the same excavation rate, more effort is transmitted to the silt than to the clay. Furthermore, silt and clay are given the same mechanical properties (Table 5). Consequently, the vertical displacements observed during the excavation in silt are slightly greater than the ones observed in clay (Figure 30).

The axial stresses developed within the tunnel lining and corresponding to the vertical displacements shown in Figure 31 are represented in Figure 32. An average was made at each location (tunnel crown, middle or invert) between the intrados and extrados values (points 1 and 1i, 2 and 2' and 3 and 3'). The compression levels reached at the end of the excavation range between 1 and 2 MPa.

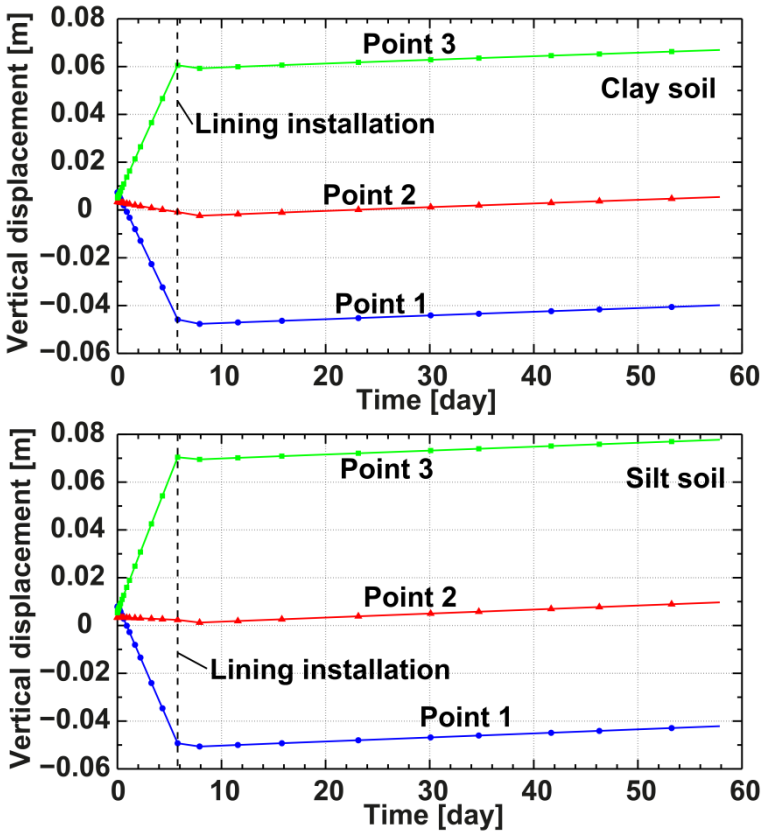

Figure 31: Evolution of the vertical displacement at the tunnel crown (point 1), tunnel middle (point 2) and tunnel invert (point 3) for clay (top) and silt (bottom) soils

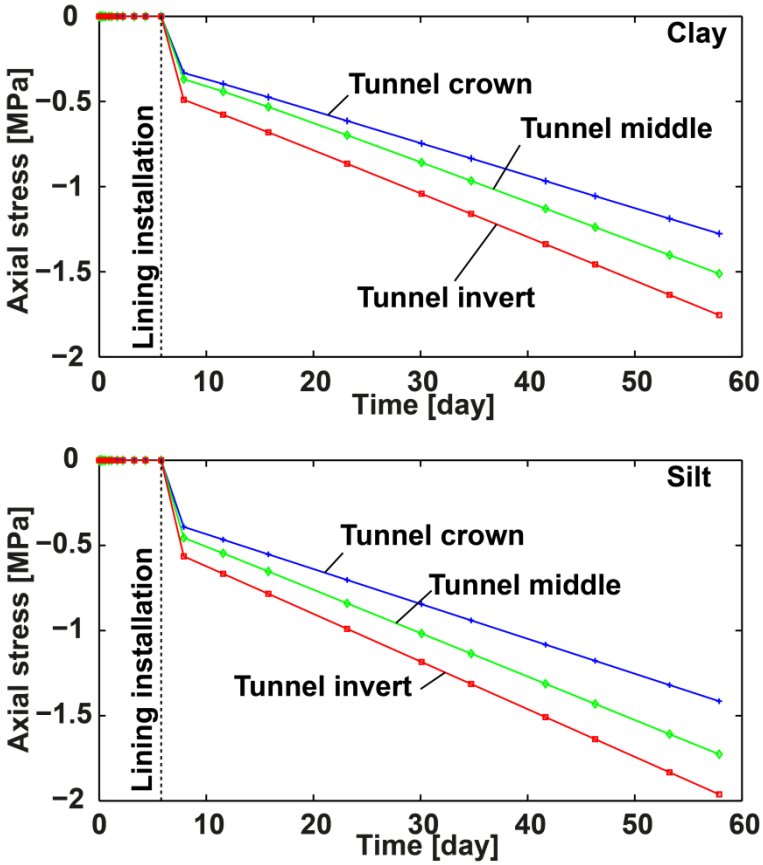

Figure 32: Axial stress development within the tunnel lining during the nodal force reduction for clay (top) and silt (bottom) soils.

Second phase: extraction and injection of heat

The optimisation of the cycles was made thanks to temperature records made at point 4 (Figure 27). The cycle Silt–Cei is taken as reference and the other cycles are given as a function of it in Table 8.

Table 8: Percentage of extracted heat compared to the most favourable situations

	Silt – Cei
Silt – Cei	100 %
Silt – Ce	77.5 %
Clay – Cei	95.0 %
Clay – Ce	65.3 %

Compared to the geometry of the cut and cover tunnel, the bored tunnel beneficiates from an increased natural heat reload capacity. Indeed, the bored tunnel nails are shorter than the cut and cover tunnel anchors so that only a “thin” layer of soil is affected but all around the tunnel structure. Thus, the gap between the linearly extracted heat for Cei cycles and Ce cycles is significantly reduced for the bored tunnel (Table 8). Obviously, longer nails would lead to a reduction of the linear extracted heat but this extraction would occur along greater distances. Nevertheless, the nails or anchors should only be design on mechanical basis, their thermal use being a plus.

The different optimisation curves representing the evolution of temperature at point 4 for the different configurations are presented in Figure 33. The optimisation carried out is made with an accuracy of 5%; that is to say if 5% more heat was extracted compared to the actual cycles given in Table 8, the temperature criteria of 274K would not be satisfied anymore.

The impact of heat injection and extraction through the tunnel nails only affects the ground

within a close vicinity of the tunnel. Indeed, large temperature variations are observed within the first tens of meters away from the tunnel lining (Figure 34).

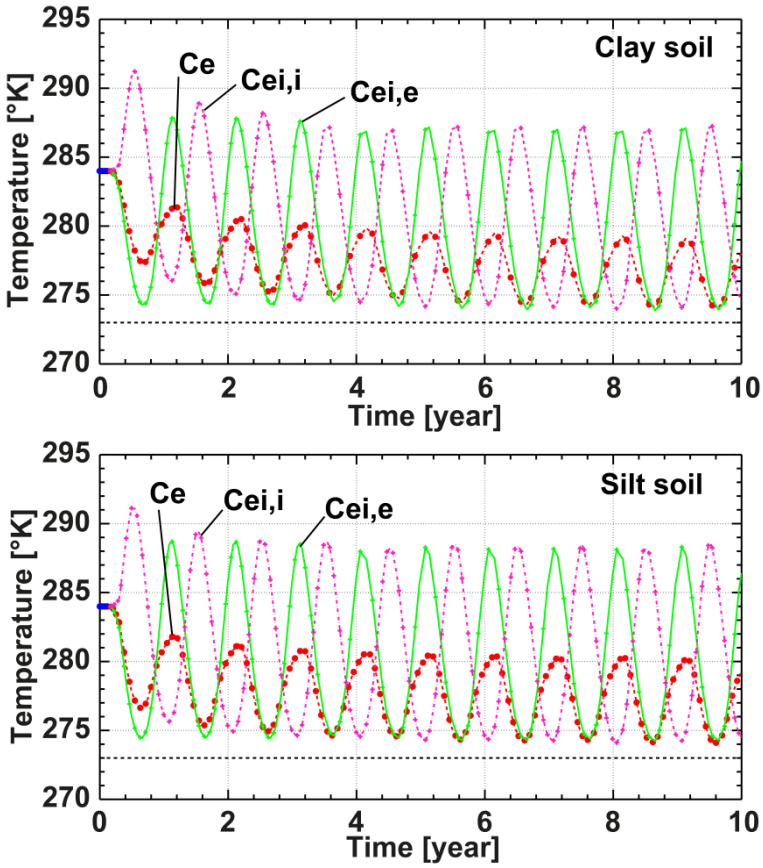

Figure 33: Time series of temperature used for the optimization of the heat exploitation cycles on clay (top) and silt (bottom). Cei,i starts with injection while Cei,e starts with extraction.

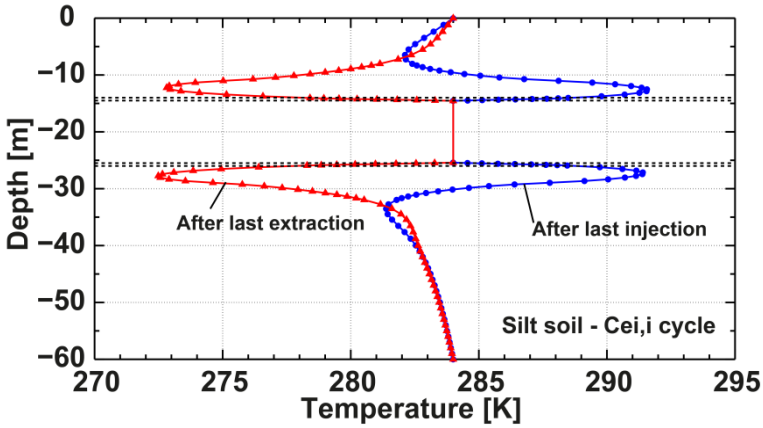

Figure 34: Profiles of temperature at the end of the last injection and extraction phases along Profile 1 for the silt soil with Cei,i cycle. If the criterion of 274K is broken here, this is because the profile goes through nails at the tunnel crown and invert.

Geotechnical impact of heat exploitation

In the present study, geotechnical issues might arise from the variations of effective stress caused by temperature variations. As the adopted model for the soil is thermoelastic, no irreversible phenomenon is observed and creeping is not investigated. Nevertheless, the thermal expansion coefficient of water is taken about 30 times greater than one for the soil/concrete (Section 3.3.3). Consequently, when the temperature increases, water expands

more than the soil matrix and excess pore water pressure is generated, reducing the effective stress accordingly. Conversely, when temperature decreases, the pore water pressure drops, increasing the effective stress accordingly. Therefore, the lining load will vary cyclically with temperature and has to be taken into account from a design standpoint.

Evolutions of axial stress on the intrados and extrados of the lining are represented in Figure 35 and Figure 36 for the Ce and Cei,i cycles, respectively. Evolutions of the stresses on the inner and outer face of the lining are in antiphase as vertical or horizontal loadings of the lining induce bending which create additional compression in the inner part of the lining and traction in the outer part of it. Thus, as Ce cycle starts with heat extraction, the load on the tunnel starts by increasing as the effective stress in the soil increases. Conversely, Cei,i starts by injecting heat which increases pore water pressure, relieving the load acting on the tunnel lining. Therefore, the axial stress observed on the lining intrados starts by being relieved while the one on the extrados increases.

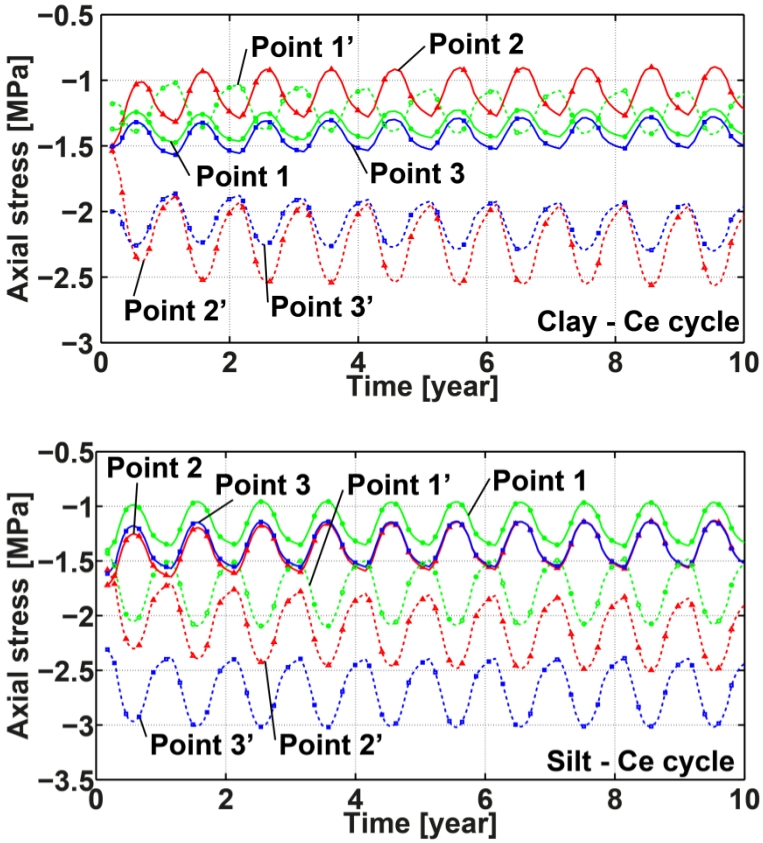

Figure 35: Time series of axial stress in the lining for clay (top) and silt (bottom) soils with Ce cycle

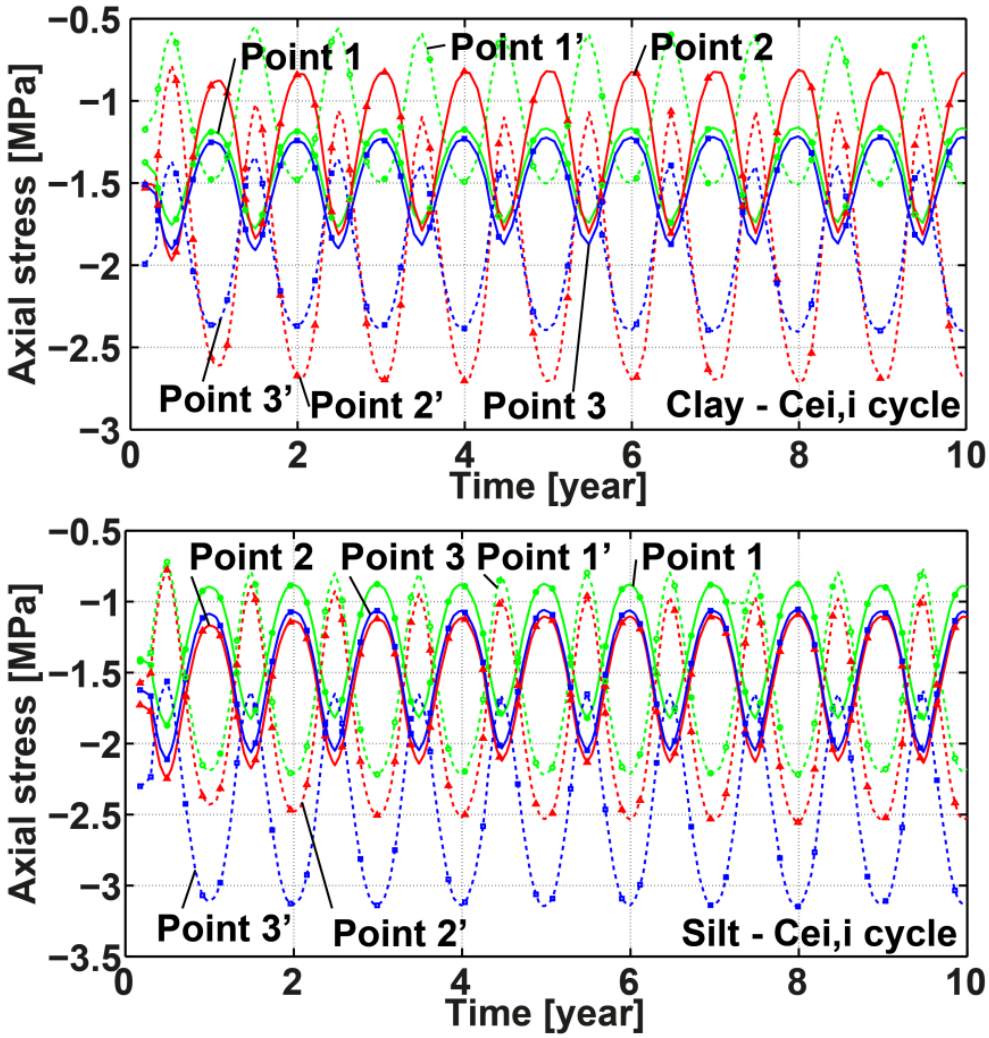

Figure 36: Time series of axial stress in the lining for clay (top) and silt (bottom) soils with Cei,i cycle

Variations in stresses observed within the tunnel lining strongly depend on the type of cycle that is considered. Indeed, if no heat injection is considered, the amplitudes of the temperature variations are reduced, resulting in stress variations of about 0.5 MPa. Furthermore, the decrease of the mean temperature leads to “permanent” stress variations as observed in Figure 35.

Heat injection induces greater temperature variations in soils leading to greater stress variations that can reach 1.5 MPa (Figure 36). The corresponding vertical displacements at points 1, 1', 3 and 3' are shown for the Ce and Cei,i cycles in Figure 37 for clay and in Figure 38 for silt. Those displacements are relative to the ones created by the excavation. Nevertheless, as the heat exploitation cycles were launched at the same moment for the two different soils and as the consolidation process was not fully achieved in clay, upward movements during the first year can be observed in clay (Figure 37, top).

Couples of points 1-1' and 3-3' exhibit the same vertical displacements and the three couples move in phase which indicates that the lining is rigid enough to move globally in one piece. Nevertheless, differences in magnitude between point couples 1-1' and points 3-3' shows that cyclic compression and dilation of the tunnel vertical diameter occurs. Indeed, the tunnel crown exhibits greater displacements than the tunnel invert, in term of magnitude. Cei,i cycle induces greater displacements compared to Ce cycle.

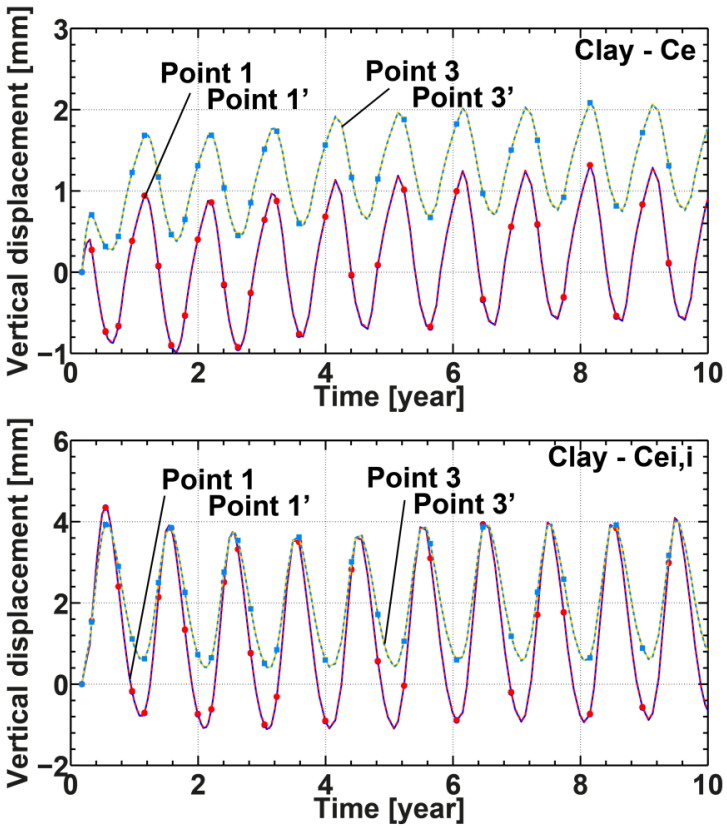

Figure 37: Vertical displacements at the tunnel crown and tunnel invert (points 1, 1', 3 and 3') for the Ce (top) and Cei,i (bottom) cycles on clay.

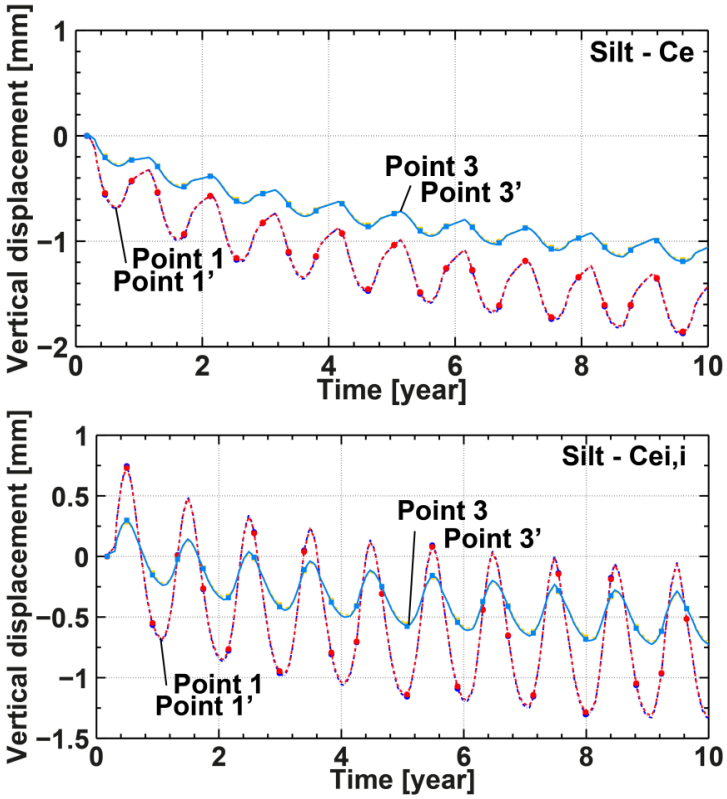

Figure 38: Vertical displacements at the tunnel crown and tunnel invert (points 1, 1', 3 and 3') for the Ce (top) and Cei,i (bottom) cycles on silt.

Variations observed in Figure 37 and Figure 38 suggest that the vertical diameter undergoes

cyclic variations which depend on the temperature variations. In the clayey soil, variations observed for the Ce cycle are between -0.5 mm and -1.1 mm while the ones observed with Cei,i cycle range from 0 mm to -1.5 mm. Those values have to be moderated by the fact that excavation should still have an impact in clay after the end of the reduction of nodal forces [30].

In the silty material, variations in diameter range from -0.2 to -0.6 mm for the Ce cycle and from +0.25 mm to -0.6 mm for the Cei,i cycle. Permanent diameter variations can be observed after the excavation as great mean temperature drops are observed in soils (Figure 33). In some cases, the diameter of the tunnel remains compressed during the heat exploitation cycles (i.e. the variation in diameter remains negative) but it can be extended as seen for the Cei,i cycle on silt, during heat injection. Thus, horizontal contraction can lead to damages on the inner structures like roadways. This is the reason why horizontal displacements around the top of the invert slab are investigated (Figure 39). As explained previously, movements during the first year of exploitation in clay are due to the consolidation process that was not fully achieved and to the thermal solicitations. Nevertheless, comparing the other years to each other, variations with amplitude ranging from 0.02 mm (Ce) to 0.1 mm (Cei,i) are observed and with a “permanent” increase of about 0.1 mm. For the silt soil, amplitudes are increased to 0.07 mm for Ce and 0.18 mm for Cei,i.

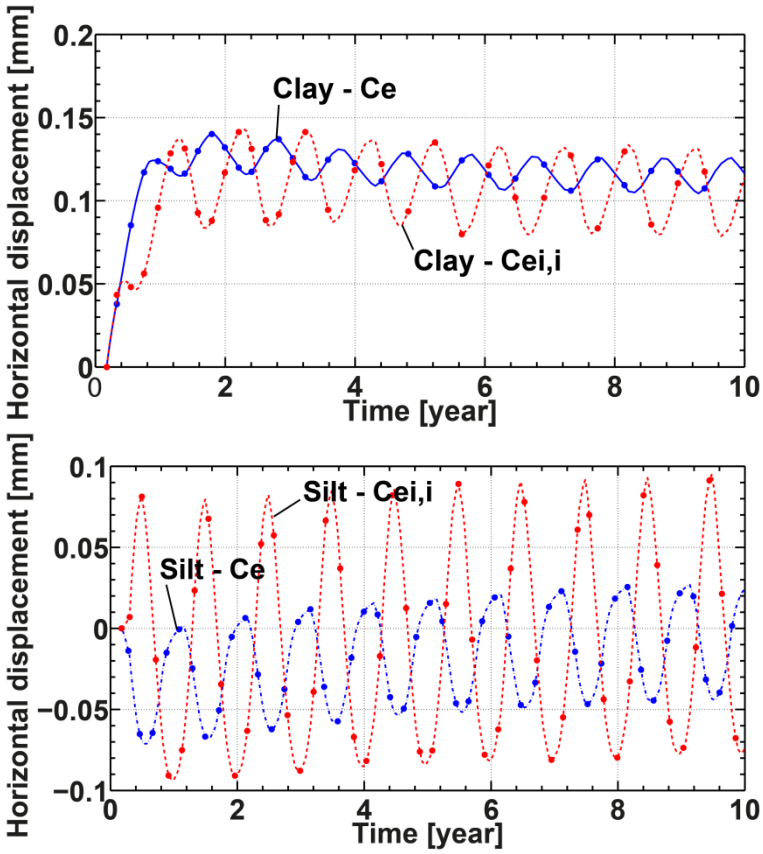

Figure 39: Horizontal displacements at the invert slab top (point 5) for Ce and Cei,i cycles in clay (top) and silt (bottom)

Finally, the vertical displacements at the soil surface on top of the tunnel crown are investigated in Figure 41. Variations in vertical displacements at point 6 are greater in clay than in silt by a factor of 4-5, reaching almost an amplitude of 1cm between -5 mm and +5 mm for the clay undergoing Cei,i cycle. Differences between Ce and Cei,i cycles are important in both soils. Cycles considering heat injection lead to greater surface displacements than cycles considering only heat extraction, by a factor of 2-3. But, it was shown that clay is a worse heat conductor than silt because its thermal diffusivity is lower. But, the greatest vertical displacements at the surface on top of the tunnel crown are observed within the soil that propagates less temperature variations. Therefore, the main parameter driving those vertical

displacements in clay is the permeability of the soil. The clay, which has the lowest permeability, undergoes greater vertical displacements that are therefore amplified by the water expansion and contraction which cannot dissipate properly. This observation was obtained with an impervious top boundary while giving a constant pressure boundary at this location could reduce this effect, this choice depending on actual urban environment at the surface. Conversely, the silt has a permeability which is high enough to prevent any significant water pressure variations. Thus, displacements observed in silt are only thermo-mechanically driven by the expansion and contraction of the soil matrix (Figure 40).

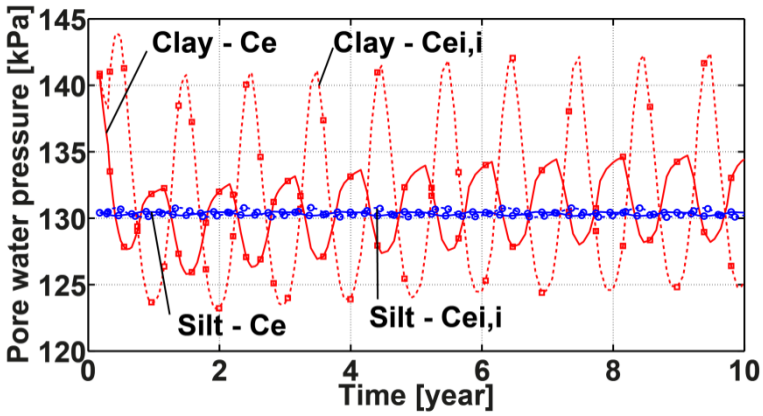

Figure 40: Pore water pressure evolution at the tunnel crown (point 1) for Ce and Cei,i cycles in clay and silt

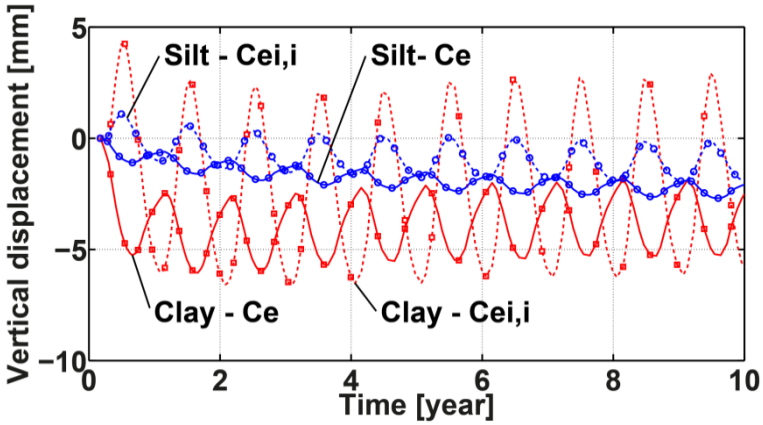

Figure 41: Vertical displacements at the soil surface just above the tunnel crown (point 6) for Ce and Cei,i cycles in clay and silt.

Estimation of the energy cost

The final energy cost is mainly driven by the difference between the extractible heat when no heat injection is considered and when it is. Thus, a good estimation of the efficiency of heat injection is to compare the difference in extracted heat between Cei and Ce cycles to the amount of injected energy which means comparing the gain to the investment, the bored tunnel having 48 meters of anchor per meter of tunnel.

For the silt soil, the gain *G* (equation (29)) represents only 35% of the injected heat while it is about 48% in the case of clay soil. As a comparison, this ratio ranges between 55% and 84% for the cut and cover tunnel. Therefore, as shown in Table 9, heat injection in silt soil is finally more expensive than using oil or gas as filling energies.

In conclusion, the bored tunnel geometry allows great natural heat reload compared to the cut and cover tunnel considered previously. Nevertheless, if the nails were longer, the extractible energy would decrease and the heat injection could become necessary.

The extractible energy per meter of tunnel and per year in the present configuration ranges from 2.8 to 3.4 MWh when no heat injection is considered and from 4.0 to 4.2 MWh when heat injection is considered.

Table 9: Energies and costs computed from the results of the bored tunnel analyses.

		Silt		Clay		Units
		Ce	Cei	Ce	Cei	
	He	45.94	57.86	38.68	54.92	(kWh/y/m of anchor)
	Hi	0.00	33.62	0.00	33.65	(kWh/y/m of anchor)
	Hf	64.32	81.00	54.15	76.89	(kWh/y/m of anchor)
Without losses	Ef	18.38	28.19	15.47	27.01	(kWh/y/m of anchor)
	Price	297.72	456.62	250.66	437.64	(cts/y/m of anchor)
	Ph	**4.63**	**5.64**	**4.63**	**5.69**	**(cts/kWh)**
	Peq (fuel oil)	**5.58**	-	**5.99**	-	(cts/kWh)
	Peq (gas)	**5.64**	-	**6.08**	-	(cts/kWh)
	Peq (Elec type VI)	**6.81**	-	**7.77**	-	(cts/kWh)
With losses	Ef	20.36	31.23	17.14	29.93	(kWh/y/m of anchor)
	Price	329.88	505.95	277.74	484.92	(cts/y/m of anchor)
	Ph	**5.13**	**6.25**	**5.13**	**6.31**	**(cts/kWh)**
	Peq (fuel oil)	**5.98**	-	**6.35**	-	(cts/kWh)
	Peq (gas)	**6.03**	-	**6.43**	-	(cts/kWh)
	Peq (Elec type VI)	**7.21**	-	**8.12**	-	(cts/kWh)
	He	**3345**	**4212**	**2816**	**3998**	**kWh / y / m of tunnel**

Cpump = 0.15 | SFP = 3.5 | Pe = 16.2 cts/kWh |P(oil) = 9.25 cts/kWh | P(gas) = 9.53 cts/kWh | P(Type VI Elec.) = 15.24 cts/kWh [24]

5 Conclusions

The potential of using anchors or nails as heat exchangers with the ground is estimated. Different configurations are investigated as the characteristics of maintaining structures (nails or anchors) vary significantly according to the tunnel structure. Few but long anchors are used to maintain the diaphragm walls during the construction of the cut and cover tunnel while numerous short nails are distributed all around the bored tunnel lining.

Furthermore, different soil conditions are investigated as the different tunnel structures reach different depths. The influence of the surface is taken into account for the cut and cover tunnel due to the proximity of the anchors but since no significant stress level is expected at this depth, the mechanical implications of heat exploitation are not investigated. Conversely, the bored tunnel reaching greater depths is assumed far enough from the soil surface to neglect it from a thermal standpoint. But the stress levels reached deeper in the ground are taken into account as great efforts on the lining are expected.

Finally, different types of heat exploitation cycles are investigated in order to estimate the pros and cons of seasonal heat exploitation. One cycle is considering heat extraction only while the two others are considering seasonal heat injection, one starting by heat injection and the other one by heat extraction.

It is found that injecting heat is economically interesting for the case of the cut and cover tunnel but not so much for the bored tunnel. Indeed, the configuration of the anchors in the cut and cover tunnel is such that they cannot beneficiate from a good natural heat reload through heat conduction. The anchors are long and on top of each other so that the used volume is great but the perimeter of this volume, which is relevant for the natural heat reload potential, is reduced. Conversely, the nails of the bored tunnel are shorter but are more numerous and distributed all around the tunnel perimeter so that the impacted volume is still important but beneficiate from an increased surface of exchange with the rest of the soil which provides a better natural heat reload. Obviously, if the nails were longer, the impacted volume would increase and the surface through which this volume is in contact with the rest of the soil would be, in proportion, reduced, impacting the efficiency of the system.

The estimated extractible heat from the present configurations ranges from 0.6 to 1.2 MWh per year and per meter of tunnel for the cut and cover tunnel, and from 2.8 to 4.2 MWh per year and per meter of tunnel for the bored tunnel. The volume of soil impacted by the heat exploitation remains in the vicinity of the anchors or nails and does not exceed a perimeter of 10 m away from the anchors and nails.

Finally, starting with heat injection or heat extraction only affects the first 3 to 5 years of the exploitation. Nevertheless, it is recommended to start by injecting heat in order to prevent freezing the soil during the first year of exploitation, or to adapt the first extraction phase if starting with it.

Mechanical implications of such heat exploitation are quantified for the bored tunnel, assuming the soil and tunnel structures behave thermoelastically. Depending on the heat exploitation cycle, variations in axial stress within the lining on the intrados and extrados range from 0.5 MPa when considering heat extraction only to 1.5 MPa when considering heat injection. Corresponding vertical and horizontal displacements were quantified and variations in vertical diameter ranged from 0 to 1.5 mm. Those diameter variations are also observed in the horizontal direction and remain around 0.1 mm close to the top of the invert slab. Shear stress within the lining is not significantly amplified by the heat exploitation. Soils having greater permeability will diffuse faster the pressure variations of water induced by temperature variations so that the mechanical implications will be reduced. Vertical displacements at the surface above the tunnel crown are not negligible as they can reach amplitudes of 1cm in clay when heat injection is considered.

In conclusion, it is shown that using the anchors or nails as heat exchangers with the soil is thermally efficient and it can provide great amount of heat for GSHP systems but that me-

chanical implications must be taken into account from a design standpoint. Experiments are needed to confirm the results (mechanical implications) that have been obtained in this study, especially in the bored tunnel. Managing the efficiency of both systems with regard to thermal losses has been shown to be an important factor in the economy of the systems, with bored tunnels showing as a better investment and a better starting point to develop the technology on an industrial scale.

6 Acknowledgements

The authors want to thank M. John Eichenberger from the Laboratory of Soil Mechanics of EPFL for his help with the German language.

Appendix

I Evolution of temperature profiles across anchors of the cut and cover tunnel

Different temperature profiles were taken along profiles 1, 2 and 3 of the cut and cover tunnel (Figure 24) for the 1st, 2nd, 5th and 9th years of exploitation, for each configuration.

I.1 Clay soil with a water table at 0m

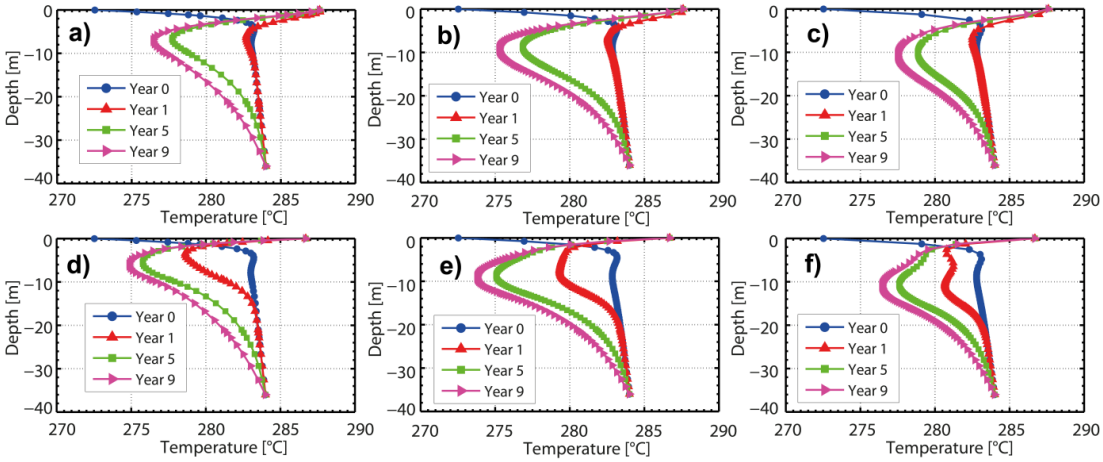

Figure A 1: Evolution of temperature profiles along profile 1 (a and d), profile 2 (b and e) and profile 3 (c and f) for the clay with a water table at 0m and undergoing Ce cycle. Figures a, b and c correspond to the end of the resting phase and figures d, e and f correspond to the end of the extraction phase.

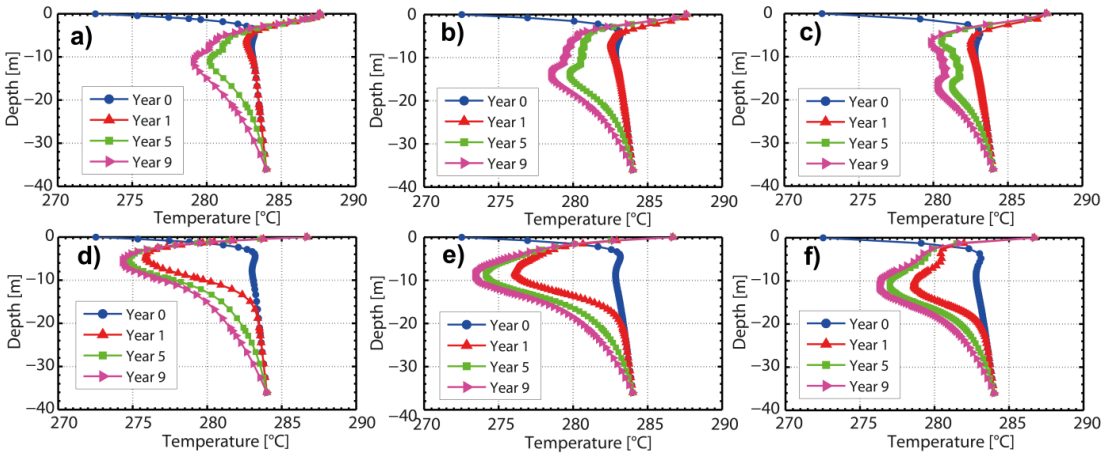

Figure A 2: Evolution of temperature profiles along profile 1 (a and d), profile 2 (b and e) and profile 3 (c and f) for the clay with a water table at 0m and undergoing Cei,e cycle. Figures a, b and c correspond to the end of the injection phase and figures d, e and f correspond to the end of the extraction phase.

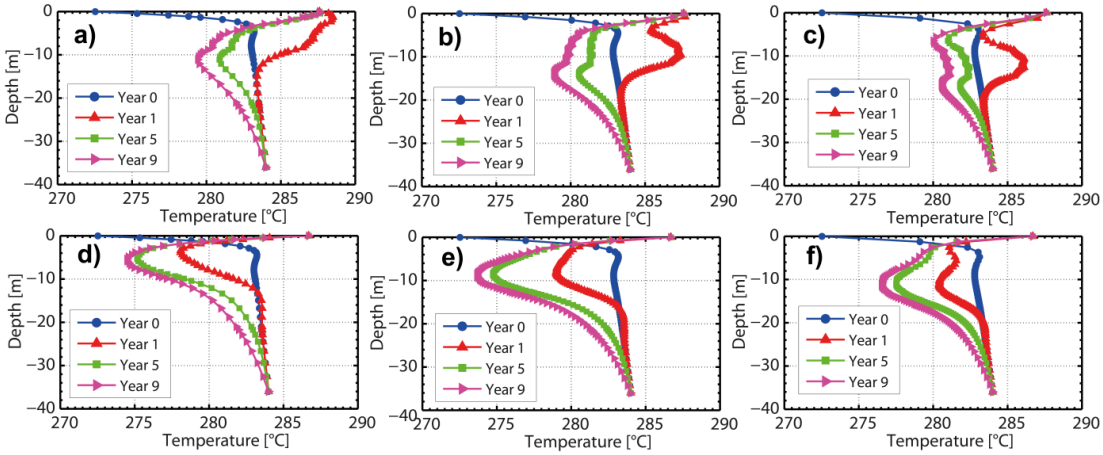

Figure A 3: Evolution of temperature profiles along profile 1 (a and d), profile 2 (b and e) and profile 3 (c and f) for the clay with a water table at 0m and undergoing Cei,i cycle. Figures a, b and c correspond to the end of the injection phase and figures d, e and f correspond to the end of the extraction phase.

I.2 Clay soil with a water table at -20m

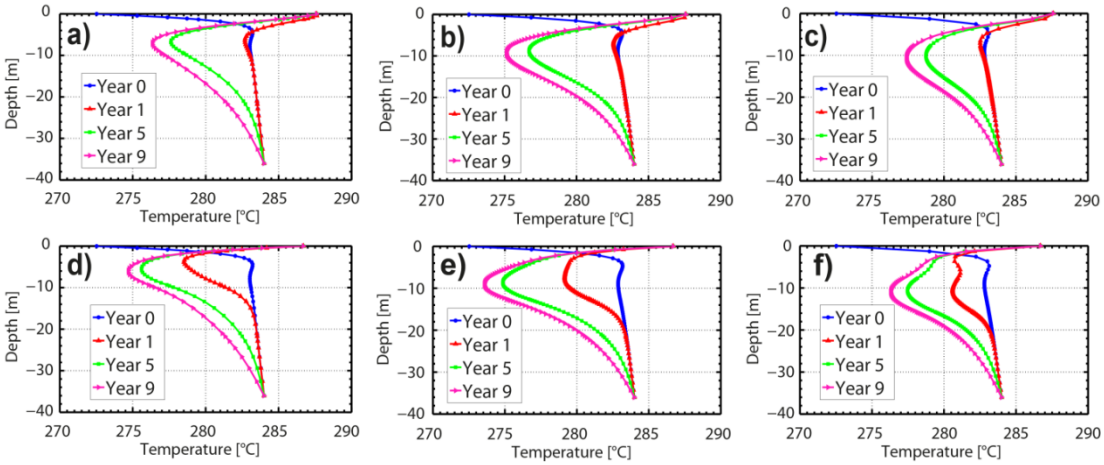

Figure 42: Evolution of temperature profiles along profile 1 (a and d), profile 2 (b and e) and profile 3 (c and f) for the clay with a water table at -20m and undergoing Ce cycle. Figures a, b and c correspond to the end of the resting phase and figures d, e and f correspond to the end of the extraction phase.

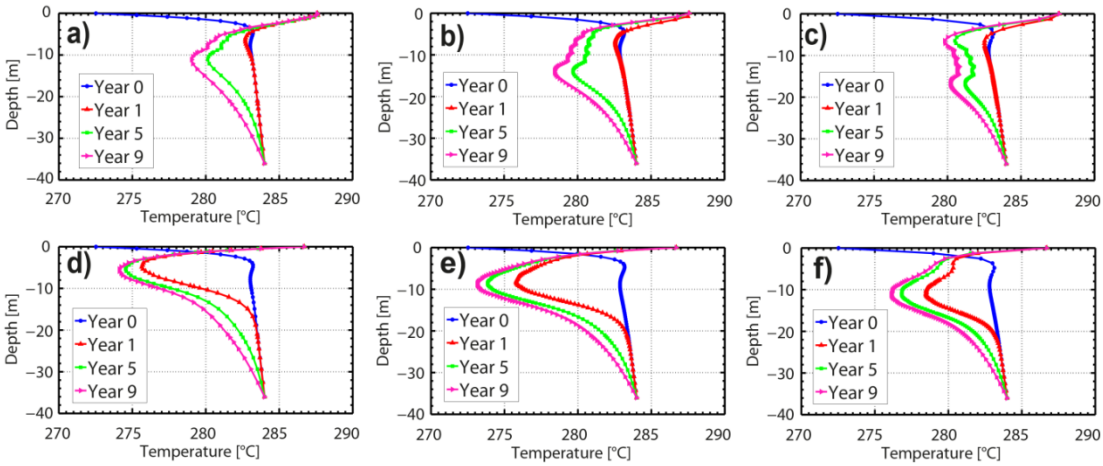

Figure 43: Evolution of temperature profiles along profile 1 (a and d), profile 2 (b and e) and profile 3 (c and f) for the clay with a water table at -20m and undergoing Cei,e cycle. Figures a, b and c correspond to the end of the injection phase and figures d, e and f correspond to the end of the extraction phase.

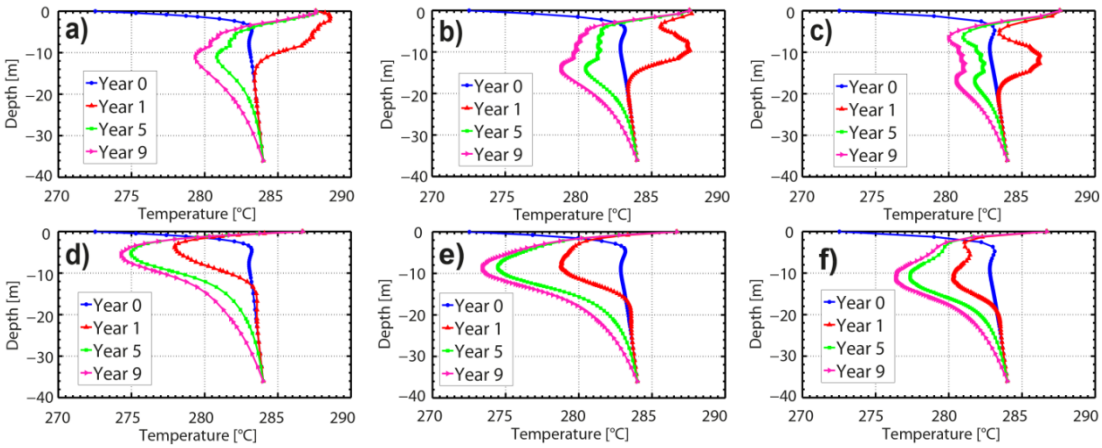

Figure 44: Evolution of temperature profiles along profile 1 (a and d), profile 2 (b and e) and profile 3 (c and f) for the clay with a water table at -20m and undergoing Cei,i cycle. Figures a, b and c correspond to the end of the injection phase and figures d, e and f correspond to the end of the extraction phase.

I.3 Silt soil with a water table at 0m

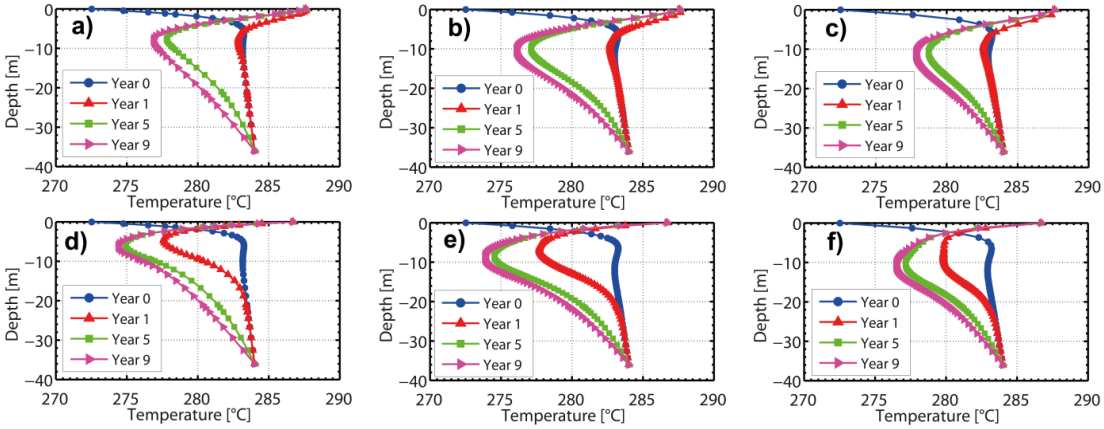

Figure A 4: Evolution of temperature profiles along profile 1 (a and d), profile 2 (b and e) and profile 3 (c and f) for the silt with a water table at 0m and undergoing Ce cycle. Figures a, b and c correspond to the end of the resting phase and figures d, e and f correspond to the end of the extraction phase.

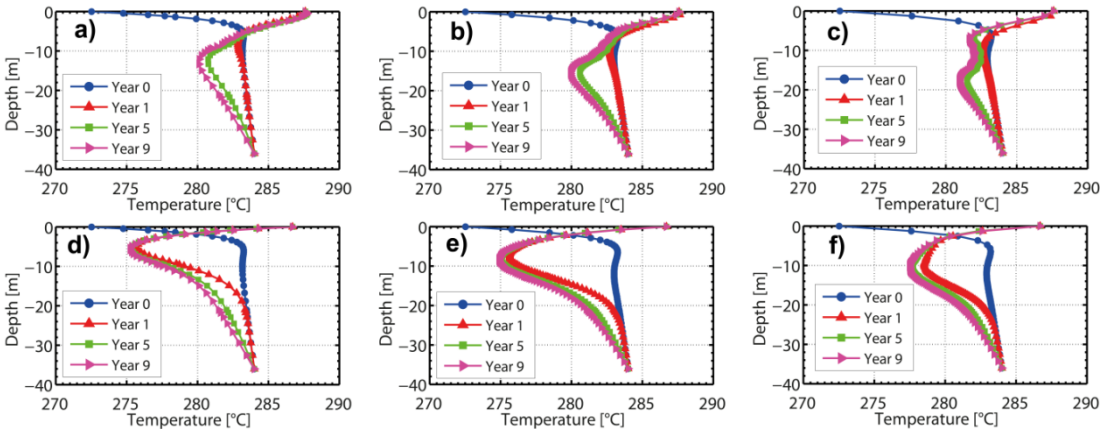

Figure A 5: Evolution of temperature profiles along profile 1 (a and d), profile 2 (b and e) and profile 3 (c and f) for the silt with a water table at 0m and undergoing Cei,e cycle. Figures a, b and c correspond to the end of the injection phase and figures d, e and f correspond to the end of the extraction phase.

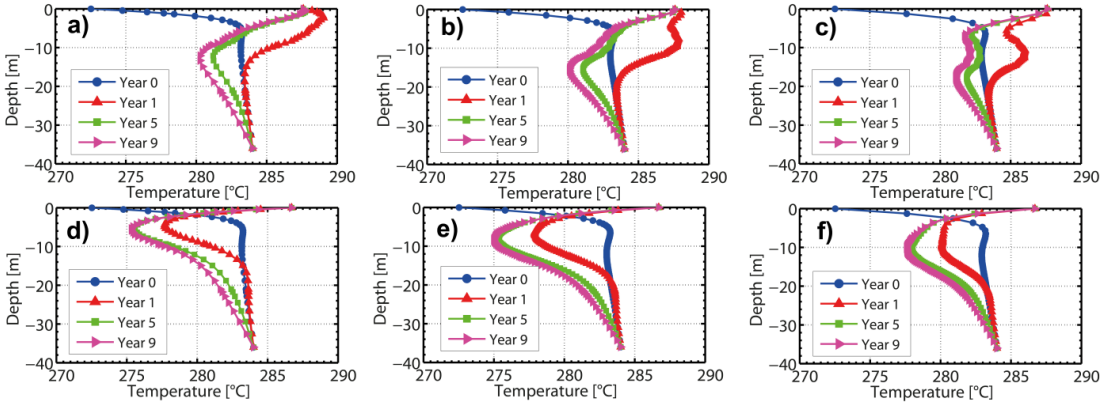

Figure A 6: Evolution of temperature profiles along profile 1 (a and d), profile 2 (b and e) and profile 3 (c and f) for the silt with a water table at 0m and undergoing Cei,i cycle. Figures a, b and c correspond to the end of the injection phase and figures d, e and f correspond to the end of the extraction phase.

I.4 Silt soil with a water table at -20m

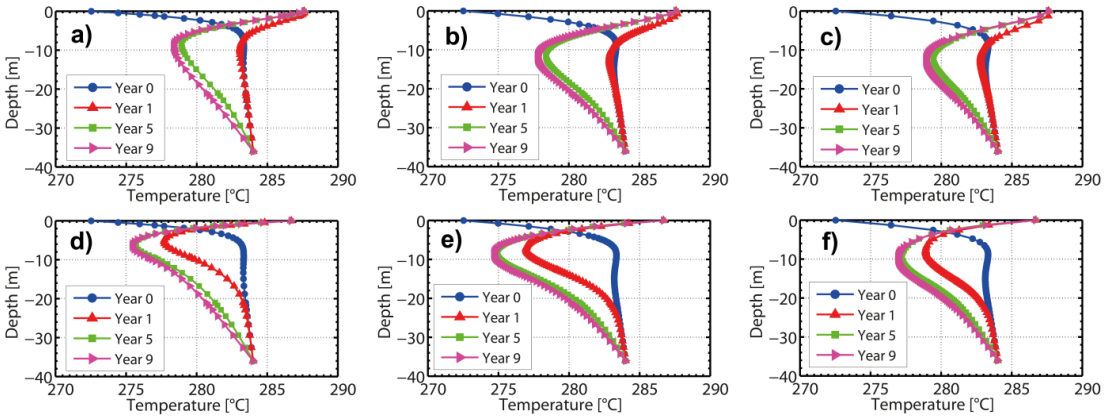

Figure A 7: Evolution of temperature profiles along profile 1 (a and d), profile 2 (b and e) and profile 3 (c and f) for the silt with a water table at -20m and undergoing Ce cycle. Figures a, b and c correspond to the end of the resting phase and figures d, e and f correspond to the end of the extraction phase.

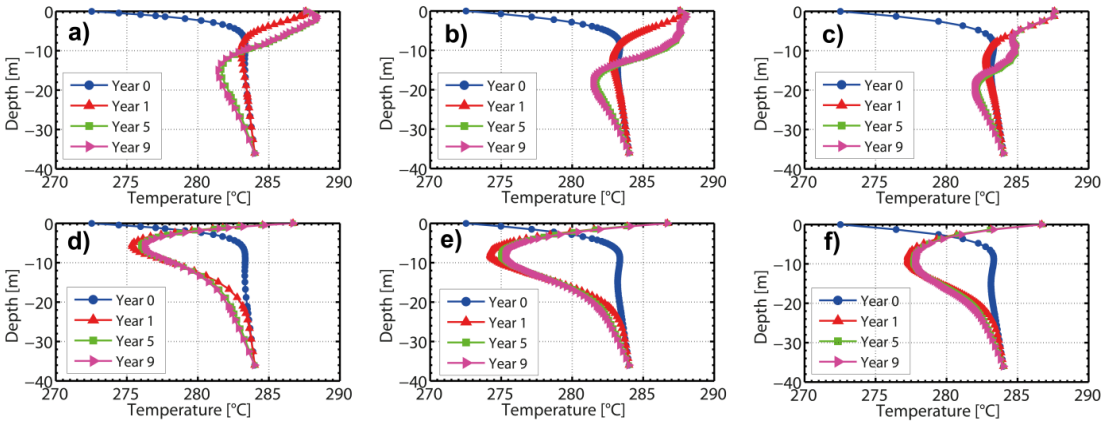

Figure A 8: Evolution of temperature profiles along profile 1 (a and d), profile 2 (b and e) and profile 3 (c and f) for the silt with a water table at -20m and undergoing Cei,e cycle. Figures a, b and c correspond to the end of the injection phase and figures d, e and f correspond to the end of the extraction phase.

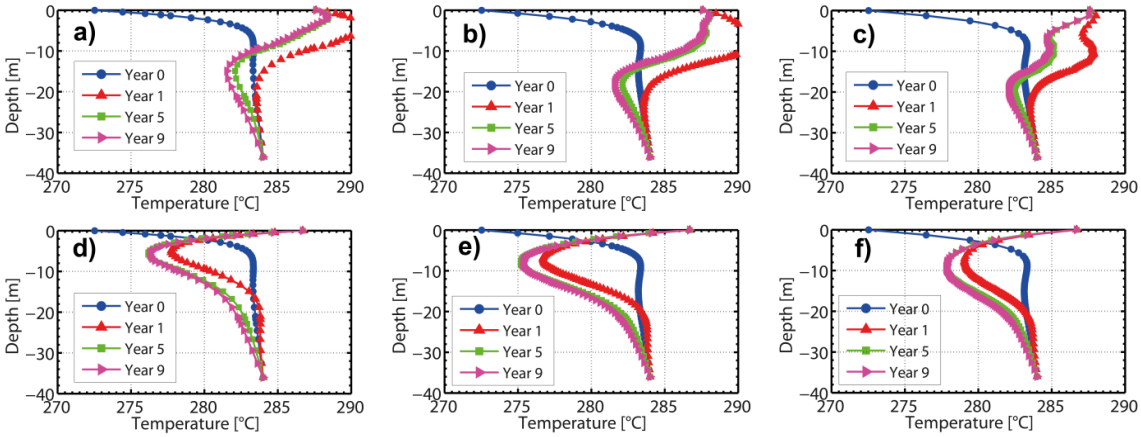

Figure A 9: Evolution of temperature profiles along profile 1 (a and d), profile 2 (b and e) and profile 3 (c and f) for the silt with a water table at -20m and undergoing Cei,i cycle. Figures a, b and c correspond to the end of the injection phase and figures d, e and f correspond to the end of the extraction phase.

II Temperature profiles around the bored tunnel

Profiles of temperature taken along profiles 1 and 3 (Figure 27) during the last year of exploitation and for the Ce and Cei,i cycles in clay are presented in Figure A 10. The succession of temperature profiles delimits the area wherein the annual temperature variations are observed. When no heat injection is considered, a zone around the tunnel from its extrados to 20 meters away from it has a permanent gap in temperature reaching its maximum of 6 degrees 3-5 meters away from the tunnel extrados. Thus, hybrid cycles could be tested on the bored tunnel. Since injecting a large amount of energy seems no so efficient from a thermal point of view because the natural heat reload is already high, one may think of injecting only the required amount of heat in order to fill each year the gap observed when no injection is considered.

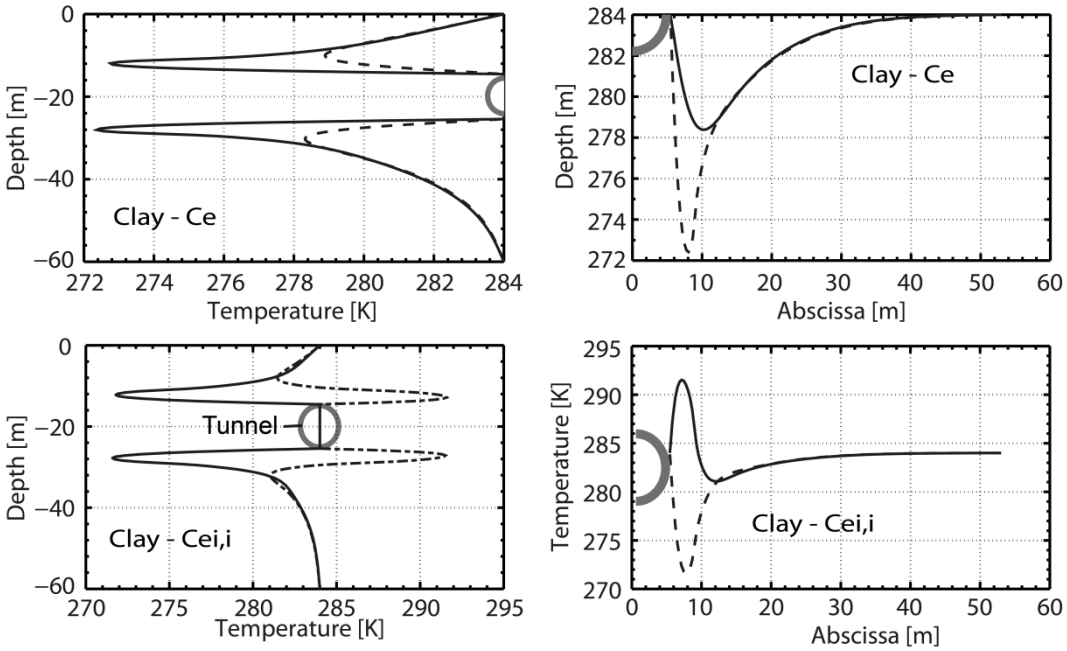

Figure A 10: Extreme vertical and horizontal profiles of temperature along profiles 1 (left panels) and profile 3 (right panels) for the Ce (top) and Cei,i (bottom) cycles in clay, after 10 years of operation.

Abbreviations

Abbreviation	Meaning
ASTRA	Bundesamt für Strassen
BFE	Bundesamt für Energie
Ce	Heat production cycle considering heat extraction only, the ground is at rest during hot periods
Cei	Heat production cycle considering heat extraction during cold periods and heat injection during cold periods
Cei,e	Cei cycle starting with heat extraction
Cei,i	Cei cycle starting with heat injection
COP	Coefficient Of Performance, comparing the energy output of a heat pump to its energy input
DATEC	Dipartimento federale dell'ambiente, dei trasporti, dell'energia e delle comunicazioni
DETEC	Département Fédéral de l'Environnement, des Transports, de l'Energie et de la Communication
FEA	Finite Element Analysis
FEM	Finite Element Method
FGU	Fachgruppe für Untertagbau
GSHP	Ground Source Heat Pump, system made of a heat pump connected to the ground through ground heat exchangers (geothermal boreholes, energy piles…)
GTS	Groupe spécialisé pour les trauvaux souterrains
He	Brut extracted heat from the ground that will be processed through the heat pump, per year
Hf	Heat output of the heat pump per year
Hi	Amount of heat injected in the ground, per year
OFEN	Office Fédérale de l'Energie
OFROU	Office Fédérale des Routes
Peq (elect type VI)	Final price of the heat when the difference to the maximum amount of heat produced is filled with type VI electricity
Peq (fuel oil)	Final price of the heat when the difference to the maximum amount of heat produced is filled with fuel oil
Peq (gas)	Final price of the heat when the difference to the maximum amount of heat produced is filled with gas
Ph	Brut price of the heat produced though the GSHP
SFP	Seasonal Factor of Perfomance, average value of COP over a year as COP depends on the season and temperature levels of heat sources
THM	Thermo-Hydro-Mechanical
UFE	Ufficio federale dell'energia
USTRA	Ufficio federale delle strade
UVEK	Departements für Umwelt, Verkehr, Energie und Kommunikation

Bibliography

[1] Infras AG Z.P.A., Basel; TEP Energy GmbH, Basics AG, Zürich Analyse des shweizerischen Energieverbrauchs 2000 – 2010 nach Verwendungszwecken. 2011.

[2] Brandl H. Energy foundations and other thermo-active ground structures. Geotechnique, 2006. 56(2): 81-122.

[3] Sanner B., Karytsas C., Mendrinos D. and Rybach L. Current status of ground source heat pumps and underground thermal energy storage in Europe. Geothermics, 2003. 32(4-6): 579-588.

[4] Florides G. and Kalogirou S. Ground heat exchangers—A review of systems, models and applications. Renewable Energy, 2007. 32(15): 2461-2478.

[5] Huttrer G.W. Geothermal heat pumps: An increasingly successful technology. Renewable Energy, 1997. 10(2-3): 481-488.

[6] Wilhelm J. and Rybach L. The geothermal potential of Swiss Alpine tunnels. Geothermics, 2003. 32(4–6): 557-568.

[7] Gonzalez R.G., Verhoef A., Vidale P.L., Main B., Gan G.G. and Wu Y.P. Interactions between the physical soil environment and a horizontal ground coupled heat pump, for a domestic site in the UK. Renewable Energy, 2012. 44: 141-153.

[8] Mustafa Omer A. Ground-source heat pumps systems and applications. Renewable and Sustainable Energy Reviews, 2008. 12(2): 344-371.

[9] Rawlings R.H.D. and Sykulski J.R. Ground source heat pumps: A technology review. Building Services Engineering Research and Technology, 1999. 20(3): 119-129.

[10] Brandl H., Adam D. and Markiewicz R. Energy geocomposites for tunnels, in *8th International Geosynthetics Conference*. 2006. Rotterdam, The Netherlands: p. 677-682.

[11] Adam D. Tunnels as Energy Sources: Technology and Case Histories, in *Tunnel*. 2008. p. 83-86.

[12] Adam D. and Markiewicz R. Energy from earth-coupled structures, foundations, tunnels and sewers. Géotechnique, 2009. 59(3): 229-236.

[13] Franzius J.N. Energy Lining Segment: design & construction for harvesting energy from TBM tunnels, in *Geothermal workshop London*. 2011. London, UK: p.

[14] Oberhauser A. Verfahrens- und Komponentenentwicklung zur Planung von Tunnelthermie- Anlagen. PhD thesis, Vienna University of Technology, 2006.

[15] Adam D. Presentation "Effizienzsteigerung durch Nutzung der Bodenspeicherung". 2008: Ringvorlesung ökologie - TU Wien.

[16] Rajeev P., Chan D. and Kodikara J. Grount-atmosphere interaction modelling for long-term prediction of soil moisture and temperature. Canadian Geotechnical Journal, 2012. 49.

[17] Bear J. and Cheng A.H.D., Modeling Groundwater Flow and Contaminant Transport. Theory and Applications of Transport in Porous Media, ed. T.-I.I.o.T. Jacob Bear: Department of Civil and Environmental Engineering, Haifa, and School of Engineering, Kinneret College oon the Sea of Galilee, Israel. Vol. 23. 2010: Springer. pp. 834.

[18] van Genuchten M.T. A closed-form equation for predicting the hydraulic conductivity of unsaturated soils. Soil Science Society of America Journal, 1980. 44(5): 892-898.

[19] Fredlung D.G. and Xing A. Equations for tghe soil-water characteristic curve. Canadian Geotechnical Journal, 1994. 31(3): 521-532.

[20] Hermansson Å., Charlier R., Collin F., Erlingsson S., Laloui L. and Sršen M., Sr., Heat Transfer in Soils, in *Water in Road Structures*, D. Andrew, Editor. 2009, Springer Netherlands. pp. 69-79.

[21] SIA-D0-190, Utilisation de la chaleur du sol par des ouvrages de fondation et de soutènement en béton. Société suisse des ingénieurs et des architectes (2005).

[22] Kovari K. and Tisa A. Computational model and charts for cut and cover tunnels, in *Colloquium tunnel structures*, I.a.f.b.a.s. engineering, Editor. 1998: Stockholm, Sweden.

[23] ISO13256-2:1998, Water-source heat pumps -- Testing and rating for performance -- Part2: Water-to-water and brine-to-water heat pumps. ISO, 1998

[24] Heizen Mit Öl. Preisvergleich Jahresmittel. 2012; Available from: http://www.erdoel-vereinigung.ch/fr/heizenmitoel/Peise/PreisvergleichJahresmittel.aspx.

[25] Collin F., Li X., Radu J.P. and Charlier R. Thermo-hydro-mechanical coupling in clay barriers. Engineering Geology, 2002. 64: 179-193.

[26] Collin F. Couplages thermo-hydro-mécaniques dans les sols et les roches tendres partiellements saturés. Université de Liège, 2003.

[27] Charlier R. Approche unifiée de quelques problèmes non linéaires de mécanique des milieux continus par la méthode des éléments finis. Université de Liège, Liège, Belgium, 1987.

[28] Charlier R., Raud J.P. and Collin F. Numerical modelling of coupled transient phenomena. Revue Française de Génie Civil, 2001. 5(6): 719-741.

[29] OFEN. Schweizerische Gesamtenergiestatistik 2011. 2012, OFEN.

[30] Potts D.M. and Zdravkovic L., Finite element analysis in geotechnical engineering: application. 2001: London: Thomas Telford. pp. 427.

[31] Panet M., Le calcul des tunnels par la méthode convergence-confinement, ed. P.d.l.E.N.d.P.e. Chaussées. 1995: Presses de l'Ecole Nationale des Ponts et Chaussées. pp. 177.

[32] Callari C. Coupled numerical analysis of strain localization induced by shallow tunnels in saturated soils. Computers and Geotechnics, 2004. 31: 193-207.

[33] Galli G., Grimaldi A. and Leonardi A. Three-dimensional modelling of tunnel excavation and lining. Computers and Geotechnics, 2004. 31(3): 171-183.

[34] Lee I.-M. and Nam S.-W. The study of seepage forces acting on the tunnel lining and tunnel face in shallow tunnels. Tunnelling and Underground Space Technology, 2001. 16(1): 31-40.

Closure of the report

Schweizerische Eidgenossenschaft
Confédération suisse
Confederazione Svizzera
Confederaziun svizra

Département fédéral de l'environnement, des transports, de l'énergie et de la communication DETEC
Office fédéral des routes OFROU

RECHERCHE DANS LE DOMAINE ROUTIER DU DETEC

Formulaire N° 3 : Clôture du projet

établi / modifié le : 03/27/2012

Données de base

Projet N° : FGU 2009-002

Titre du projet : Heat exchanger anchors for thermo-active tunnels

Echéance effective :

Textes :

Résumé des résultats du projet :

Heat exchanger geo-structures make use of existing underground construction elements to use them as heat-exchanger. Anchors used for underground construction can be used as such, as prototypes of coaxial heat-exchanger anchors have been made. As is usual with direct heat production, the consumer and the site must be closely located, and this has oriented the case studies towards urban tunnels rather than deep tunnels. Two cases have been evaluated, one being a cut-and-cover tunnel and the second a shallow bored tunnel. These construction cases can be realised in a variety of soils exhibiting various thermo-hydro-mechanical characteristics.

Different combinations of construction type and soil nature have been modelled in order to evaluate the possibilities regarding energy production and mechanical consequences.
The characteristics of possible sites, as well as technology on both the anchor side and the heat-pump side are first studied. Finite-element method simulations using parameters derived from this study are used to identify the most favorable techniques, in terms of soil nature, tunnel type, exploitation strategy. Pure heat extraction is tested against heat extraction and injection cycles that are currently growing in interest in the shallow geothermal energy community. Both structural and economic analysis is performed.

Results highlight that the shallow bored tunnel is the best of the two solutions, allowing around 3 MWh of heat being extracted per meter of tunnel each year, without thermal reload, and at low estimated prices. Variations observed in tunnel lining stresses due to temperature cycles as well as surface displacements are found to be significant: up to 0.9 MPa additional compressive stress in the lining and vertical displacement cycles with an amplitude of 5 mm at the surface. Additional care should be taken regarding the built environment, as well as the inner structures of the tunnel that also undergo horizontal deformations, though of lesser magnitude. The cut-and-cover tunnel is less favorable due to the geometry of the anchors placement combined with the proximity of the surface, leading to a maximum extraction of 0.8 MWh/m/yr and increasing the time before the investment is recouped. It is nevertheless better adapted to thermal reload, multiplying the usable energy by a factor up to two and if such an usage is needed can become advantageous.

Schweizerische Eidgenossenschaft
Confédération suisse
Confederazione Svizzera
Confederaziun svizra

Département fédéral de l'environnement, des transports, de l'énergie et de la communication DETEC
Office fédéral des routes OFROU

Atteinte des objectifs :

The objective of evaluating the feasibility from both economic and geotechnical points of view has been achieved: cost of a variety of cases has been calculated on the basis of simulations and existing systems, and the identification of geotechnical problems has been performed. State-of-the-art thermo-hydro-mechanical simulations were used in order to achieve this objective of combining knowledge from both the geotechnical and the geothermal point of views. Some specificities of tunnel anchors were not taken into account in the proposal. Being detached from the structure after the construction period is over, studying anchor friction during heat cycles was deemed unnecessary, leading to an analysis differing from energy piles. It is then the efforts induced by thermal solicitation in the tunnel lining that are evaluated (milestone 5). Finally recommendations for prototype projects have been made on the basis of the study.

Déductions et recommandations :

The recommendations regarding the use of tunnel anchors as heat-exchangers are to prefer a shallow bored tunnel with anchor stabilisation. This type of structure promises higher returns for similar initial cost and a simpler strategy regarding energy use through the year. The counterpart is that it can influence not only the built environment on the surface but also the structure itself, leading to the need of dimensioning the lining to this solicitation. Inner dimensional variations should also be taken into account for all elements inside the tunnel (slab, road surface, fixed equipments) Cut-and-cover tunnel structure is unaffected due to the presence of the buffering backfill, but the built environment is affected and its efficiency with regard to the initial cost is lower.

Publications :

Report FGU 2009-02.
Conférence Journée technique du LAVOC 2010: Utilisation des structures géotechniques pour l'extraction d'énergie dans les routes.

Chef/cheffe de projet :

Nom : Laloui Prénom : Lyesse

Service, entreprise, institut : Laboratoire de mécanique des sols, ENAC, EPFL

Signature du chef/de la cheffe de projet :

Schweizerische Eidgenossenschaft
Confédération suisse
Confederazione Svizzera
Confederaziun svizra

Département fédéral de l'environnement, des transports, de l'énergie et de la communication DETEC
Office fédéral des routes OFROU

RECHERCHE DANS LE DOMAINE ROUTIER DU DETEC

Formulaire N° 3 : Clôture du projet

Appréciation de la commission de suivi :

Evaluation :

Die Beurteilung der BK bzgl. Zielerreichung und Interpretation der Modellaussagen stimmt mit jener der Forschungsstelle überein.

Mise en oeuvre :

Die erzielten Ergebnisse zeigen die grundsätzliche Machbarkeit der Energiegewinnung aus thermoaktiven Ankern insbesondere bei bergmännisch aufgefahrenen Tunnels und können als eine wichtige Grundlage für die Planung einer Pilotanlage in der Zukunft betrachtet werden. Allfällige Synergien mit dem geplanten Forschungsprojekt FGU 2012-005 sollten genutzt werden.

Besoin supplémentaire en matière de recherche :

Dieser besteht bzgl. Validierung im Feld im Rahmen einer Pilotanlage oder eines Grossversuchs.

Influence sur les normes :

Keiner.

Président/Présidente de la commission de suivi :

Nom : Anagnostou Prénom : Georgios

Service, entreprise, institut : ETH Zürich

Signature du président/ de la présidente de la commission de suivi :

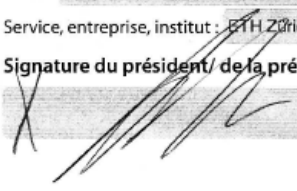

Index of research reports on roads

Forschungsberichte seit 2009

Bericht-Nr.	Projekt Nr.	Titel	Datum
1356	SVI 2007/014	Kooperation an Bahnhöfen und Haltestellen *Coopération dans les gares et arrêts* *Coopération at railway stations and stops*	2011
1362	SVI 2004/012	Aktivitätenorientierte Analyse des Neuverkehrs Activity oriented analysis of induced travel demand Analyse orientée aux acitivtés du trafic induit	2012
1361	SVI 2004/043	Innovative Ansätze der Parkraukmbewirtschaftung Approches innovantes de la gestion du stationnement Innovative approaches to parking management	2012
1357	SVI 2007/007	Unaufmerksamkeit und Ablenkung: Was macht der Mensch am Steuer? Driver Inattention and Distraction as Cause of Accident: How do Drivers Behave in Cars? L'inattention et la distraction: comment se comportent les gens au volant?	2012
1360	VSS 2010/203	Akustische Führung im Strassentunnel Acoustical guidance in road tunnels Guidage acoustique dans les tunnels routiers	2012
1365	SVI 2004/014	Neue Erkenntnisse zum Mobilitätsverhalten dank Data Mining? De nouvelles découvertes sur le comportement de mobilité par Data Mining? New findings on the mobility behavior through Data Mining?	2011
1359	SVI 2004/003	Wissens- und technologientransfer im Verkehrsbereich Know-how and technology transfer in the transport sector Transfert de savoir et de technologies dans le domaine des transports	2012
1363	VSS 2007/905	Verkehrsprognosen mit Online -Daten Pronostics de trafic avec des données en temps réel Traffic forecast with real-time data	2011
1367	VSS 2005/801	Grundlagen betreffend Projektierung, Bau und Nachhaltigkeit von Anschlussgleisen Principes de bases concernant la conception, la construction et la durabilité de voies de raccordement Basic Principles on the Design, Construction and Sustainability of Sidings	2011
1370	VSS 2008/404	Dauerhaftigkeit von Betongranulat aus Betongranulat	2011
1373	VSS 2008/204	Vereinheitlichung der Tunnelbeleuchtung	2012
1369	VSS 2003/204	Rétention et traitement des eaux de chaussée	2012

648	AGB 2005/023 + AGB 2006/003	Validierung der AAR-Prüfungen für Neubau und Instandsetzung	2011
1371	ASTRA 2008/017	Potenzial von Fahrgemeinschaften *Potentiel du covoiturage* *Potential of Car Pooling*	2011
1374	FGU 2004/003	Entwicklung eines zerstörungsfreien Prüfverfahrens für Schwiessnähte von KDB *Dévelopment d'une méthode d'éssais non-déstructif pour des soudures de membranes polymères d'étanchéité* *Development of a nondestructive test method for welded seams of polymeric sealing membranes*	2012
1375	VSS 2008/304	Dynamische Signalisierungen auf Hauptverkehrsstrassen *Signalisations dynamiques sur des routes principales* *Dynamic signalling at primary distributors*	2012
1376	ASTRA 2011/008_004	Erfahrungen im Schweizer Betonbrückenbau *Expériences dans la construction de ponts en Suisse* *Experiences in Swiss Bridge Construction*	2012
1379	VSS 2010/206_OBF	Harmonisierung der Abläufe und Benutzeroberflächen bei Tunnel-Prozessleitsystemen *Harmonisation of procedures and user interface in Tunnel-Process Control Systems* *Harmonisation des processus et des interfaces utilisateurs dans les systèmes de supervision de tunnels*	2012
1380	ASTRA 2007/009	Wirkungsweise und Potential von kombinierter Mobilität *Mode of action and potential of combined mobility* *Mode d'action et le potentiel de la mobilité combinée*	2012
1381	SVI 2004/055	Nutzen von Reisezeiteinsparungen im Personenverkehr *Bénéfices liés à une réduction des temps de parcours du trafic voyageur* *Benefits of travel time savings in passenger traffic*	2012
1383	FGU 2008/005	Einfluss der Grundwasserströmung auf das Quellverhalten des Gipskeupers im Chienbergtunnel *Influence de l'écoulement souterrain sur le gonflement du Keuper gypseux dans le Tunnel du Chienberg* *Influence of groundwater flow on the swelling of the Gipskeuper formation in the Chienberg tunnel*	2012
1386	VSS 2006/204	Schallreflexionen an Kunstbauten im Strassenbereich *Réflexions du trafic routier aux ouvrages d'art* *Noise reflections on structures in the street*	2012

1387	VSS 2010/205_OBF	Ablage der Prozessdaten bei Tunnel-Prozessleitsystemen *Data storage in tunnel process control systems* *Enregistrement ds données de systèmes de supervision de tunnels*	2012
649	AGB 2008/012	Anforderungen an den Karbonatisierungswiderstand von Betonen *Exigences par rapport à la résistance à la carbonatationdes bétons* *Requirements for the carbonation resistance of concrete mixes*	2012
650	AGB 2005/010	Korrosionsbeständigkeit von nichtrostenden Betonstählen *Résistance à la corrosion des aciers d'armature inoxydables* *Use of stainless steels in concrete structures*	2012